EpCAM-Positive Hepatocellular Carcinoma Cells Are Tumor-Initiating Cells With Stem/Progenitor Cell Features

TARO YAMASHITA,* JUNFANG JI,* ANURADHA BUDHU,* MARSHONNA FORGUES,* WEN YANG,‡ HONG-YANG WANG,‡ HULIANG JIA,§ QINGHAI YE,§ LUN-XIU QIN,§ ELAINE WAUTHIER,‖ LOLA M. REID,‖ HIROSHI MINATO,¶ MASAO HONDA,¶ SHUICHI KANEKO,¶ ZHAO-YOU TANG,§ and XIN WEI WANG*

*Liver Carcinogenesis Section, Laboratory of Human Carcinogenesis, Center for Cancer Research, National Cancer Institute, Bethesda, Maryland; ‡International Cooperation Laboratory on Signal Transduction, Eastern Hepatobiliary Surgery Institute, Shanghai, China; §Liver Cancer Institute and Zhongshan Hospital, Fudan University, Shanghai, China; ‖Department of Cell and Molecular Physiology, University of North Carolina School of Medicine, Chapel Hill, North Carolina; and the ¶Liver Disease Center and Kanazawa University Hospital, Kanazawa University, Kanazawa, Japan

Background & Aims: **Cancer progression/metastases and embryonic development share many properties including cellular plasticity, dynamic cell motility, and integral interaction with the microenvironment. We hypothesized that the heterogeneous nature of hepatocellular carcinoma (HCC), in part, may be owing to the presence of hepatic cancer cells with stem/progenitor features.** ***Methods:*** **Gene expression profiling and immunohistochemistry analyses were used to analyze 235 tumor specimens derived from 2 recently identified HCC subtypes (EpCAM$^+$ α-fetoprotein [AFP$^+$] HCC and EpCAM$^-$ AFP$^-$ HCC). These subtypes differed in their expression of AFP, a molecule produced in the developing embryo, and EpCAM, a cell surface hepatic stem cell marker. Fluorescence-activated cell sorting was used to isolate EpCAM$^+$ HCC cells, which were tested for hepatic stem/progenitor cell properties.** ***Results:*** **Gene expression and pathway analyses revealed that the EpCAM$^+$ AFP$^+$ HCC subtype had features of hepatic stem/progenitor cells. Indeed, the fluorescence-activated cell sorting–isolated EpCAM$^+$ HCC cells displayed hepatic cancer stem cell–like traits including the abilities to self-renew and differentiate. Moreover, these cells were capable of initiating highly invasive HCC in nonobese diabetic, severe combined immunodeficient mice. Activation of Wnt/β-catenin signaling enriched the EpCAM$^+$ cell population, whereas RNA interference-based blockage of EpCAM, a Wnt/β-catenin signaling target, attenuated the activities of these cells.** ***Conclusions:*** **Taken together, our results suggest that HCC growth and invasiveness is dictated by a subset of EpCAM$^+$ cells, opening a new avenue for HCC cancer cell eradication by targeting Wnt/β-catenin signaling components such as EpCAM.**

Tumors originate from normal cells as a result of accumulated genetic/epigenetic changes. Although considered monoclonal in origin, tumor cells are heterogeneous in their morphology, clinical behavior, and molecular profiles.[1,2] Tumor cell heterogeneity has been explained previously by the clonal evolution model[3]; however, recent evidence has suggested that heterogeneity may be owing to derivation from endogenous stem/progenitor cells[4] or de-differentiation of a transformed cell.[5] This hypothesis supports an early proposal that cancers represent "blocked ontogeny"[6] and a derivative that cancers are transformed stem cells.[7] This renaissance of stem cells as targets of malignant transformation has led to realizations about the similarities between cancer cells and normal stem cells in their capacity to self-renew, produce heterogeneous progenies, and limitlessly divide.[8] The cancer stem cell (CSC) (or tumor-initiating cell) concept is that a subset of cancer cells bear stem cell features that are indispensable for a tumor. Accumulating evidence suggests the involvement of CSCs in the perpetuation of various cancers including leukemia, breast cancer, brain cancer, prostate cancer, and colon cancer.[9–13] Experimentally, putative CSCs have been isolated using cell surface markers specific for normal stem cells. Stem cell–like features of CSC have been confirmed by functional in vitro clonogenicity and in vivo tumorigenicity assays. For example, leukemia-initiating cells in nonobese diabetic, severe combined immunodeficient (NOD/SCID) mice are CD34^{++}CD38$^-$.[11] Breast cancer CSCs are CD44$^+$CD24$^{-/low}$ cells, whereas tumor-initiating cells of the brain, colon, and prostate are CD133$^+$.[10,12,13] CSCs are considered more metastatic and drug-/radiation-resistant than non-CSCs in the tumor, and are responsible for cancer relapse. These findings warrant the development of treatment strategies that can specifically eradicate CSCs.[14,15]

Abbreviations used in this paper: AFP, α-fetoprotein; BIO, 6-bromoindirubin-3′-oxime; CSC, cancer stem cell; FACS, fluorescence-activated cell sorting; 5-FU, 5-fluorouracil; HpSC, hepatic stem cell; IF, immunofluorescence; IHC, immunohistochemistry; MACS, magnetic-activated cell sorting; MeBIO, 1-methyl-BIO; MH, mature hepatocyte; PCNA, proliferating cell nuclear antigen; siRNA, small interfering RNA.

0016-5085/09/$36.00
doi:10.1053/j.gastro.2008.12.004

Hepatocellular carcinoma (HCC) is the third leading cause of cancer death worldwide.[16] Although the cellular origin of HCC is unclear,[17,18] HCC has heterogeneous pathologies and genetic/genomic profiles,[19] suggesting that HCC can initiate in different cell lineages.[20] The liver is considered as a maturational lineage system similar to that in the bone marrow.[21] Experimental evidence indicates that certain forms of hepatic stem cells (HpSCs), present in human livers of all donor ages, are multipotent and can give rise to hepatoblasts,[22,23] which are, in turn, bipotent progenitor cells that can progress either into hepatocytic or biliary lineages.[22,24] α-fetoprotein (AFP) is one of the earliest markers detected in the liver bud specified from the ventral foregut,[25,26] but its expression has been found only in hepatoblasts and to a lesser extent in committed hepatocytic progenitors, not in later lineages or in normal human HpSC.[22] Recent studies also have indicated that EpCAM is a biomarker for HpSC because it is expressed in HpSCs and hepatoblasts.[22-24]

We recently identified a novel HCC classification system based on EpCAM and AFP status.[27] Gene expression profiles revealed that EpCAM$^+$ AFP$^+$ HCC (referred to as *HpSC-HCC*) has progenitor features with poor prognosis, whereas EpCAM$^-$ AFP$^-$ HCC (referred to as *mature hepatocyte-like HCC*; MH-HCC) have adult hepatocyte features with good prognosis. Wnt/β-catenin signaling, a critical player for maintaining embryonic stem cells,[28] is activated in EpCAM$^+$ AFP$^+$ HCC, and EpCAM is a direct transcriptional target of Wnt/β-catenin signaling.[29] Moreover, EpCAM$^+$ AFP$^+$ HCC cells are more sensitive to β-catenin inhibitors than EpCAM$^-$ HCC cells in vitro.[29] Interestingly, a heterogeneous expression of EpCAM and AFP was observed in clinical tissues, a feature that may be attributed to the presence of a subset of CSCs. In this study, we have confirmed that EpCAM$^+$ HCC cells are highly invasive and tumorigenic, and have activated Wnt/β-catenin signaling. We also show a crucial role of EpCAM in the maintenance of hepatic CSCs. Our data shed new light on the pathogenesis of HCC and may open new avenues for therapeutic interventions for targeting hepatic CSCs.

Materials and Methods

Clinical Specimens

HCC samples were obtained with informed consent from patients who underwent radical resection at the Liver Cancer Institute of Fudan University, Eastern Hepatobiliary Surgery Institute, and the Liver Disease Center of Kanazawa University Hospital, and the study was approved by the institutional review boards of the respective institutes. The microarray data from clinical specimens are available publicly (GEO accession number, GSE5975).[27] Array data from a total of 156 HCC cases (155 hepatitis B virus [HBV]-positive) corresponding to 2 subtypes of HCC (ie, HpSC-HCC and MH-HCC), were used to search for HpSC-HCC–associated genes (Supplementary Table 1; see supplementary material online at www.gastrojournal.org). A total of 79 formalin-fixed and paraffin-embedded HCC samples were used for immunohistochemistry (IHC) analyses (Supplementary Table 2; see supplementary material online at www.gastrojournal.org), 56 of which also were used in a recent study.[30] The classification of HpSC-HCC and MH-HCC was based on previously described criteria.[27]

Cell Cultures and Sorting

Human liver cancer cell lines (HuH1 and HuH7) were derived from Health Science Research Resources Bank (JCRB0199 and JCRB0403, respectively) and routinely cultured as previously described.[31] Normal human MHs, provided by the University of Pittsburgh through Liver Tissue Cell Distribution System, were cultured as previously described.[32] Human HpSCs were isolated from fetal livers and cultured in Kubota and Reid's[33] medium as previously described. Wnt10B conditioned medium was prepared as described.[34] Embryonic stem cell culture medium was prepared using Knockout Dulbecco's modified Eagle medium supplemented with 18% of Serum Replacement (Invitrogen, Carlsbad, CA). The pTOPFLASH and pFOP-FLASH luciferase constructs were described previously.[29] BIO and MeBIO were generous gifts from Ali Brivanlou (The Rockefeller University, New York, NY). For isolating single cell–derived colonies to determine whether heterogeneity is an intrinsic property of EpCAM$^+$ cells, HuH1 and HuH7 cells were resuspended and plated as a single cell per well in 96-well plates. A total of 192 single cells were plated successfully. The clones that grew well were selected 2 weeks after seeding and used for immunofluorescence (IF) analysis. The 5-fluorouracil (5-FU) stock (2 mg/mL; Sigma, St Louis, MO), was prepared in distilled water. Fluorescence-activated cell sorting (FACS) and magnetic-activated cell sorting (MACS) analyses were used to isolate EpCAM$^+$ HCC cells (Supplementary materials; see supplementary Materials and Methods online at www.gastrojournal.org).

Clonogenicity, Spheroid Formation, Invasion, Quantitative Reverse Transcription–Polymerase Chain Reaction, and IHC Assays

For colony formation assays, 2000 EpCAM$^+$ or EpCAM$^-$ cells were seeded in 6-well plates after FACS. After 10 days of culture, cells were fixed by 100% methanol and stained with methylene blue. For spheroid assays, single-cell suspensions of 1000 EpCAM$^+$ or EpCAM$^-$ cells were seeded in 6-well Ultra-Low Attachment Microplates (Corning, Corning, NY) after FACS. The number of spheroids was measured 14 days after seeding. Invasion assays were performed using BD BioCoat Matrigel Matrix Cell Culture Inserts and Control Inserts (BD Biosciences, San Jose, CA) essentially as pre-

viously described.[31] Reverse transcription–polymerase chain reaction and IHC assays are described in detail in the supplementary materials (see supplementary material online at www.gastrojournal.org).

Tumorigenicity in NOD/SCID Mice

Six-week-old NOD/SCID mice (NOD/NCrCRl-*Prkdc*^{scid}) were purchased from Charles River (Charles River Laboratories, Inc, Wilmington, MA). The protocol was approved by the National Cancer Institute–Bethesda Animal Care and Use Committee. Cells were suspended in 200 μL of Dulbecco's modified Eagle medium and Matrigel (1:1), and a subcutaneous injection was performed. The size and incidence of subcutaneous tumors were recorded. For histologic evaluation, tumors were formalin-fixed, paraffin-embedded or embedded directly in OCT compound (Sakura Finetek, Torrance, CA) and stored at −80°C.

RNA Interference

A small interfering RNA (siRNA) specific to *TACSTD1* (SI03019667) and a control siRNA (1022076) were designed and synthesized by Qiagen (Qiagen, Valencia, CA). Transfection was performed using Lipofectamine 2000 (Invitrogen), according to the manufacturer's instructions. A total of 200 nmol/L of siRNA duplex was used for each transfection.

Statistical Analyses

The class comparison and gene clustering analyses were performed as previously described.[30] The canonic pathway analysis was performed using Ingenuity Pathways Analysis (v5.5; Ingenuity Systems, Redwood City, CA). The association of HCC subtypes and clinicopathologic characteristics was examined using either the Mann–Whitney *U* test or the chi-square test. Student *t* tests were used to compare various test groups assayed by colony formation, spheroid formation, or invasion assays. The Kaplan–Meier survival analysis was performed to compare patient survival or tumorigenicity.

Results

A Poor Prognostic HCC Subtype With Molecular Features of HpSC

We re-evaluated the gene expression profiles that were uniquely associated with 2 recently identified prognostic subtypes of HCC (ie, HpSC-HCC and MH-HCC), using a publicly available microarray dataset of 156 HCC cases (GEO accession number: GSE5975). Sixty cases were defined as HpSC-HCC with a poor prognosis and 96 cases were defined as MH-HCC with a good prognosis, based on EpCAM and AFP status.[27] A class-comparison analysis with univariate *t* tests and a global permutation test (1000×) yielded 793 genes that were expressed differentially between HpSC-HCC and MH-HCC ($P < .001$). Hierarchical cluster analyses revealed 2 main gene clusters that were up-regulated (cluster A; 455 genes) or down-regulated (cluster B; 338 genes) in HpSC-HCC (Figure 1*A*). Pathway analysis indicated that the enriched genes in cluster A were associated significantly with known stem cell signaling pathways such as transforming growth factor-β, Wnt/β-catenin, PI3K/Akt, and integrin ($P < .01$) (Figure 1*B*). In contrast, genes in cluster B were associated significantly with mature hepatocyte functions such as xenobiotic metabolism, complement system, and coagulation system ($P < .01$). Noticeably, known HpSC markers such as *KRT19* (CK19), *TACSTD1* (EpCAM), *AFP*, *DKK1*, *DLK1*, and *PROM1* (CD133) were up-regulated significantly in HpSC-HCC, whereas known liver maturation markers such as *UGT2B7* and *CYP3A4* were expressed more abundantly in MH-HCC (Figure 1*C* and Supplementary Tables 3 and 4; see supplementary material online at www.gastrojournal.org). Kaplan–Meier survival analysis revealed that HpSC-HCC patients had a significantly shorter survival than MH-HCC patients ($P = .036$) (Figure 1*D*). Consistently, HpSC-HCC patients had a high frequency of macroscopic and microscopic portal vein invasion (Figure 1*E*).

However, IHC analyses of an additional 79 HCC cases revealed that among 24 HpSC-HCC cases, EpCAM staining was very heterogeneous with a mixture of EpCAM$^+$ and EpCAM$^-$ tumor cells in each tumor (Figure 1*F*, *left panel*). Noticeably, many of the EpCAM$^+$ tumor cells were located at the invasion border zones and often were disseminated at the invasive front (*black arrows*). IF analysis revealed that HCC cells located at the invasive front co-expressed EpCAM, CK19, and AFP (Figure 1*F*, *right panels*). Noticeably, HpSC-HCC patients were significantly younger than MH-HCC patients (Supplementary Tables 1 and 2; see supplementary material online at www.gastrojournal.org). Enrichment of EpCAM$^+$ AFP$^+$ tumor cells at the tumor-invasive front suggested their involvement in HCC invasion and metastasis.

Isolation and Characterization of EpCAM$^+$ Cells in HCC

The results described earlier suggest that HpSC-HCC may be organized in a hierarchical fashion in which EpCAM$^+$ tumor cells act as stem-like cells with an ability to differentiate into EpCAM$^-$ tumor cells. To test this hypothesis, we first evaluated the expression pattern of 7 hepatic stem/maturation markers (EpCAM, CD133, CD90, CK19, Vimentin, Hep-Par1, and β-catenin) in 6 HCC cell lines (Figure 2*A*). All 3 AFP$^+$ cell lines (HuH1, HuH7, and Hep3B) expressed EpCAM, CD133, and cytoplasmic/nuclear β-catenin, whereas the other 3 AFP$^-$ cell lines (SK-Hep-1, HLE, and HLF) did not, consistent with the microarray data. Interestingly, AFP$^+$ cell lines had no CD90$^+$ cell population, which recently was identified as hepatic CSCs,[35] whereas AFP$^-$ cell lines had such a population. Consistent with the IF data, FACS analysis showed that AFP$^+$ cell lines had a subpopulation of

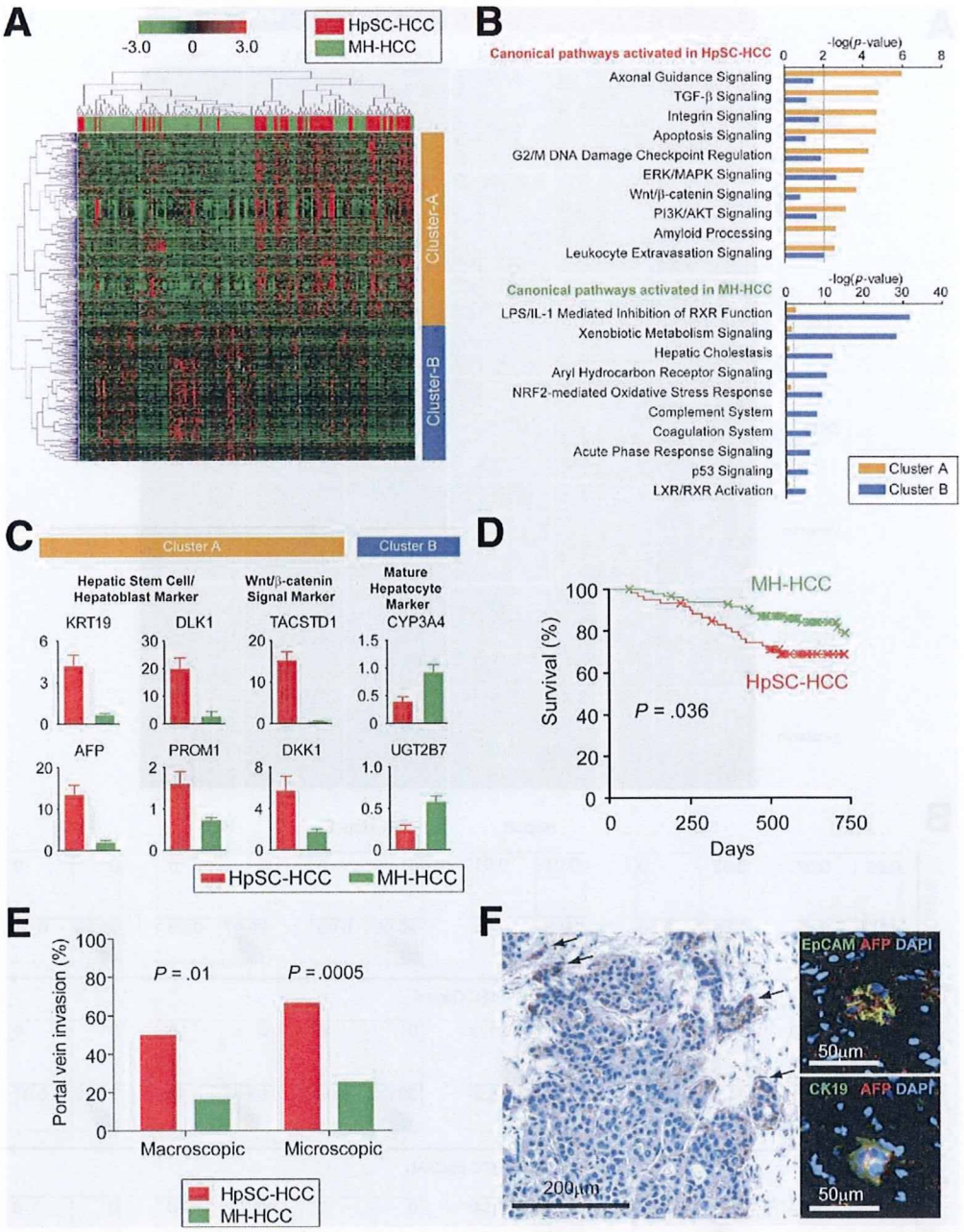

Figure 1. HpSC–HCC represents a subset of invasive HCCs with CSC features. (*A*) Hierarchical cluster analysis based on 793 HpSC–HCC–coregulated genes in 156 HCC cases. Each cell in the matrix represents the expression level of a gene in an individual sample. Red and green cells depict high and low expression levels, respectively, as indicated by the scale bar. (*B*) Pathway analysis of HpSC–HCC–coregulated genes. The top 10 canonical signaling pathways activated in cluster A (*upper panel*) or cluster B (*lower panel*) with statistical significance ($P < .01$) are shown. (*C*) Expression patterns of well-known HpSC and MH markers in each HCC subtype as analyzed by microarray. (*D*) Kaplan–Meier survival analysis of the cases used for array analysis. (*E*) Frequency of macroscopic and microscopic portal vein invasion in HpSC-HCC and MH-HCC used for IHC. (*F*) Representative images of EpCAM, AFP, and CK19 staining in HpSC–HCC samples analyzed by IHC and IF. EpCAM staining illustrates heterogeneous expression of EpCAM in HpSC-HCC (*left panel*). EpCAM$^+$ cells were disseminated in the invasive border (*left panel black arrows*) with expression of AFP (*right top panel*) and CK19 (*right bottom panel*).

EpCAM$^+$ and CD133$^+$, but no CD90$^+$ cells, whereas AFP$^-$ cell lines had a subpopulation of CD90$^+$ cells but no EpCAM$^+$ or CD133$^+$ cells (Figure 2*B*). These data indicate that HpSC-HCC and MH-HCC cell lines have distinct stem cell marker expression patterns, and EpCAM as well as CD133 may be hepatic CSC markers specifically in HpSC-HCC.

We selected 2 human HCC cell lines (HuH1 and HuH7) to isolate EpCAM$^+$ cells because both lines were heterogeneous in EpCAM, AFP, CK19, and β-catenin expression (Figure 2*A* and *B* and Supplementary Figure 1*A*; see supplementary material online at www.gastrojournal.org).[29] We successfully enriched EpCAM$^+$ and EpCAM$^-$ populations from HuH7 cells by FACS, with more than 80% purity in EpCAM$^+$ cells and more than 90% purity in EpCAM$^-$ cells 1 day after sorting (Figure 3*A*). Similar results were obtained when the purity check was performed immediately after sorting (data not shown). EpCAM$^+$ cells also were positive for CK19 and β-catenin (Figure 3*B* and Supplementary Figure 1*B*; see supplementary material online at www.gastrojournal.org) and most were AFP$^+$ (data not shown). In contrast, EpCAM$^-$ cells were negative for these markers but positive for HepPar1, a monoclonal antibody specific to hepatocytes (Figure 3*B*). Consistent with the microarray data described earlier, the levels of *TACSTD1*, *MYC*, and *hTERT* (known HpSC markers) were increased significantly in EpCAM$^+$ HuH7 cells, whereas the levels of *UGT2B7* and *CYP3A4*

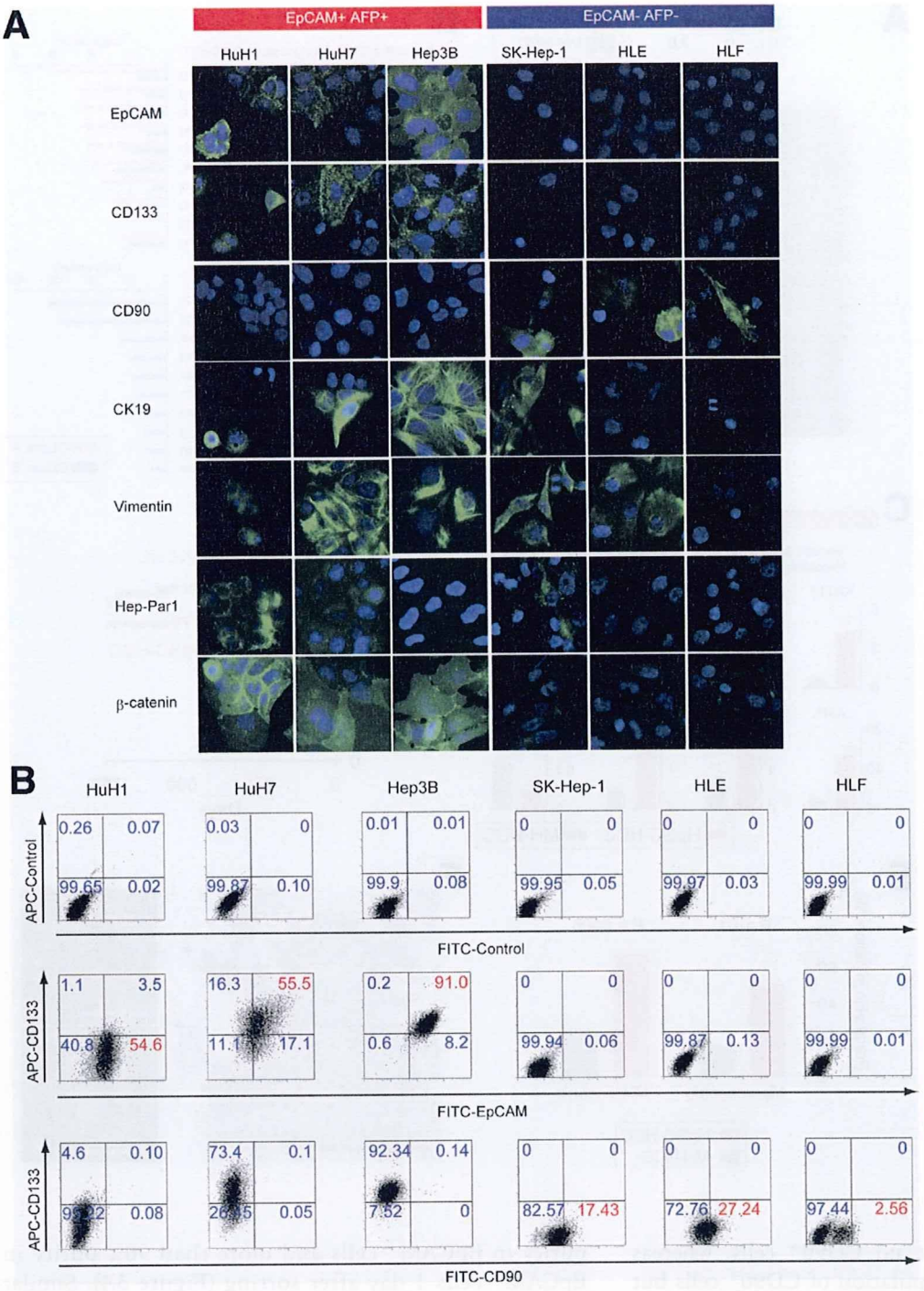

Figure 2. Characterization of hepatic stem cell marker expression in HCC cell lines. (*A*) IF analysis of 6 HCC cell lines (EpCAM$^+$ AFP$^+$ cell lines: HuH1, HuH7, and Hep3B; EpCAM$^-$ AFP$^-$ cell lines: SK-Hep-1, HLE, and HLF) stained with anti-EpCAM, anti-CD133, anti-CD90, anti-CK19, anti-Vimentin, anti–Hep-Par1, and anti–β-catenin antibodies. (*B*) FACS analysis of 6 HCC cell lines stained with anti-EpCAM, anti-CD133, and anti-CD90 antibodies.

(known mature hepatocyte markers) were significantly higher in EpCAM$^-$ HuH7 cells (Figure 3*C*, *left upper panel*). This expression pattern was reminiscent of human HpSC cells (Figure 3*C*, *left lower panel*). Similar results were obtained from HuH1 cells (data not shown). We also compared gene expression patterns of isolated HuH1, HuH7, MH, and HpSC cells using the TaqMan Human Stem Cell Pluripotency Array (Applied Biosystems, Foster City, CA) containing 96 selected human stem cell–related genes. Although a differential expression pattern of stem cell–related genes was evident among HpSC, EpCAM$^+$ HuH1, and EpCAM$^+$ HuH7 cells, the EpCAM$^+$ HCC cells were related more closely to HpSC cells whereas EpCAM$^-$ HCC cells were related more closely to diploid adult mature hepatocytes (Figure 3*C*, *right panel*; and Supplementary Figure 1C; see supplementary material online at www.gastrojournal.org). Thus, it appeared that EpCAM$^+$ HCC cells had a gene expression pattern that is related more closely to HpSC than EpCAM$^-$ HCC cells.

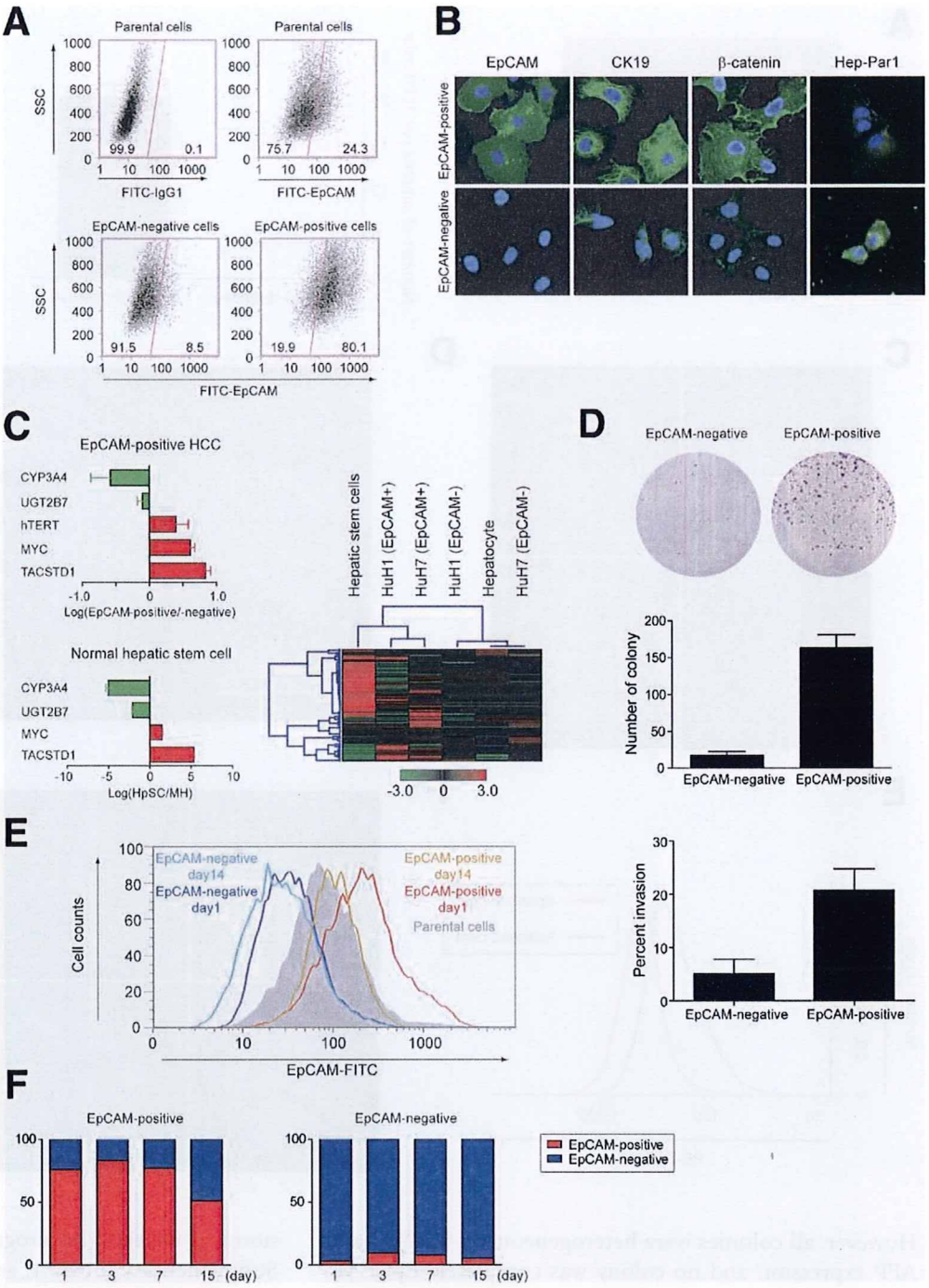

Figure 3. Characterization of EpCAM$^+$ and EpCAM$^-$ cells in HuH7 cells. (*A*) FACS analysis of EpCAM$^+$ and EpCAM$^-$ cells on day 1 after cell sorting. (*B*) IF analysis of cells stained with anti-EpCAM, anti-AFP, anti-CK19, or anti-β-catenin antibodies. (*C*) Quantitative reverse-transcription polymerase chain reaction analysis of EpCAM$^+$ and EpCAM$^-$ HuH7 cells (*left upper panel*) or HpSCs and MHs (*left lower panel*). Experiments were performed in triplicate. Hierarchical cluster analysis of HpSC, MH, and EpCAM$^+$ and EpCAM$^-$ HCC cells using a panel of genes expressed in human embryonic stem cells (*right panel*). Gene expression was measured in quadruplicate. (*D*) Representative photographs of the plates containing colonies derived from 2000 EpCAM$^+$ or EpCAM$^-$ HuH7 cells (*upper panel*). Colony formation experiments were performed in triplicate (mean ± SD) (*middle panel*). Cell invasiveness of EpCAM$^+$ and EpCAM$^-$ cells using the Matrigel invasion assay (*lower panel*). (*E*) Flow cytometer analysis of EpCAM$^+$ and EpCAM$^-$ HuH7 cells stained with anti-EpCAM at days 1 and 14 after cell sorting. (*F*) Percentage of sorted EpCAM$^+$ and EpCAM$^-$ cells after culturing for various times as analyzed by IF. Numbers of EpCAM$^+$ and EpCAM$^-$ cells were counted in 3 independent areas of chamber slides at days 1, 3, 7, and 15 after cell sorting. The average percentages of EpCAM$^+$ or EpCAM$^-$ cells are depicted as *red* or *blue*, respectively.

The isolated EpCAM$^+$ HuH7 cells formed colonies efficiently whereas EpCAM$^-$ cells failed to do so (Figure 3*D*, *upper* and *middle panels*; and Supplementary Figure 2*A* for HuH1 cells; see supplementary material online at www.gastrojournal.org). In addition, EpCAM$^+$ HuH7 cells were much more invasive than EpCAM$^-$ cells ($P < .03$) (Figure 3*D*, *lower panel*; and Supplementary Figure 2*B* for HuH1 cells; see supplementary material online at www.gastrojournal.org). The EpCAM$^+$ fraction decreased with time in sorted EpCAM$^+$ HuH7 cells from greater than 80% to 50% (Figure 3*E*). However, a small percentage of EpCAM$^+$ cells remained constant in sorted EpCAM$^-$ HuH7 cells. FACS analysis confirmed the results of IF analysis (Figure 3*F* and Supplementary Figure 2*C* for HuH7 and HuH1 cells, respectively; see supplementary material online at www.gastrojournal.org), suggesting that EpCAM$^+$ cells could differentiate into EpCAM$^-$ cells, eventually allowing an enriched EpCAM$^+$ fraction to revert back to parental cells after 14 days of culture. In contrast, EpCAM$^-$ cells maintained their EpCAM$^-$ status. In addition, we successfully isolated 12 HuH1 and 2 HuH7 colonies from 192 single-cell–plated culture wells.

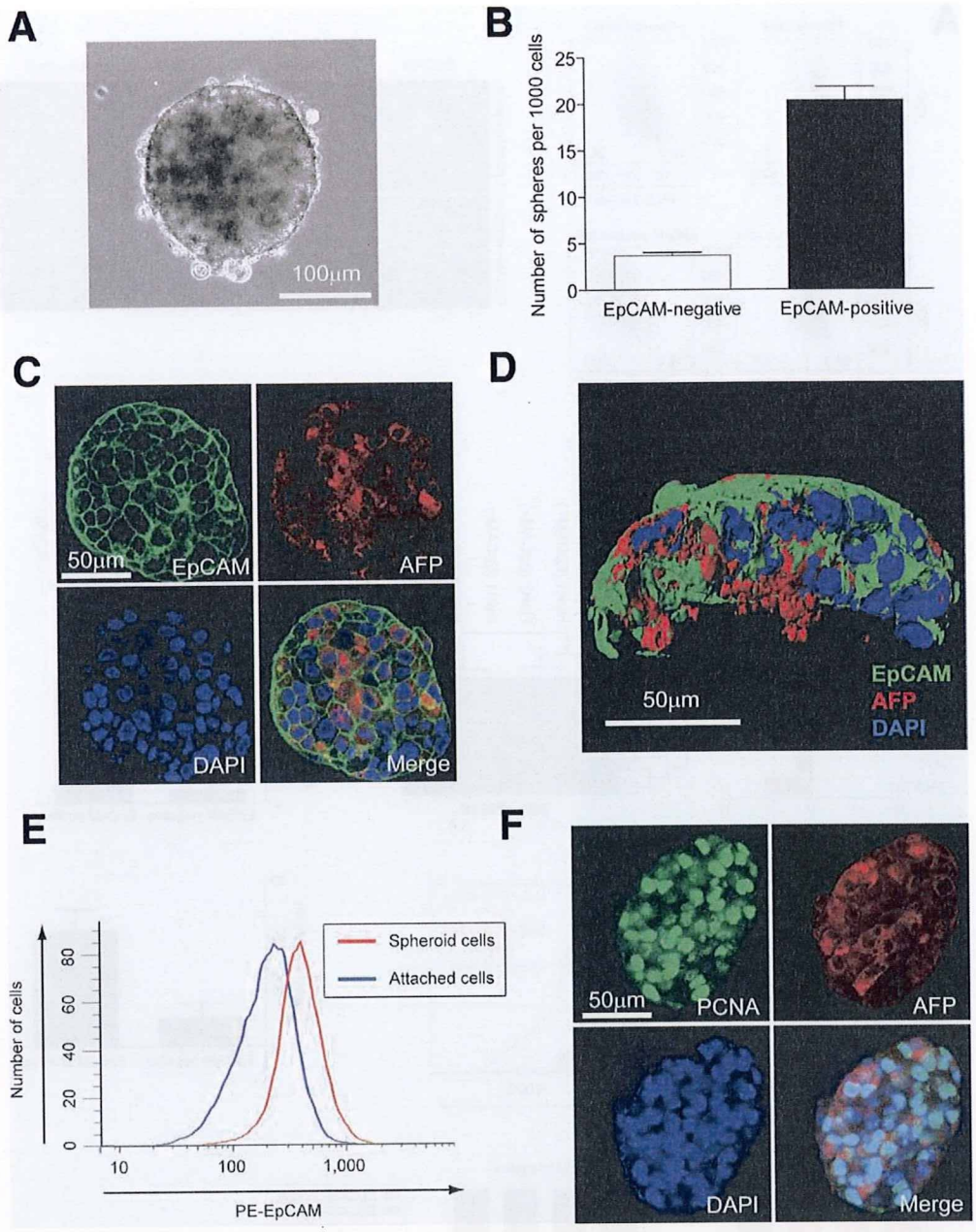

Figure 4. Spheroid formation of EpCAM$^+$ HuH1 HCC cells. (*A*) A representative phase-contrast image of an HCC spheroid derived from an EpCAM$^+$ cell (*scale bar*, 100 μm) and (*B*) total numbers of spheroids from 1000 sorted cells are shown. Experiments were performed in triplicate and data are shown as mean ± SD. (*C*) Representative confocal images of an HCC spheroid co-stained with anti-EpCAM, anti-AFP, and 4′,6-diamidino-2-phenylindole (DAPI) (*scale bar*, 50 μm). (*D*) A 3-dimensional image of an HCC spheroid co-stained with anti-EpCAM, anti-AFP, and DAPI (*scale bar*, 50 μm) reconstructed from confocal images using surface rendering. (*E*) FACS analysis of EpCAM$^+$ cells cultured as spheroid cells (*red*) or attached cells (*blue*) for 14 days after cell sorting. (*F*) Confocal images of an HCC spheroid co-stained with anti-PCNA, anti-AFP, and DAPI (*scale bar*, 50 μm).

However, all colonies were heterogeneous in EpCAM and AFP expression and no colony was completely EpCAM$^-$ (data not shown). Taken together, these results indicate that EpCAM$^+$ HCC cells resemble HpSC features. It appears that EpCAM$^+$ cells, but not EpCAM$^-$ cells, have self-renewal and differentiation capabilities with the ability to form colonies from a single cell, and produce both EpCAM$^+$ and EpCAM$^-$ cells.

It has been shown previously that stem/progenitor cells and cancer stem/progenitor cells can form spheroids in vitro in a nonattached condition.[36,37] Consistently, EpCAM$^+$ cells could form spheroids efficiently, reaching to about 150 to approximately 200 μm in diameter after 14 days of culture (Figure 4*A* and *B*). Interestingly, all cells in a spheroid were EpCAM$^+$, whereas AFP expression was relatively heterogeneous (Figure 4*C* and *D*, and Supplementary movie 1; see supplementary material online at www.gastrojournal.org). Rarely, a few spheroids derived from an EpCAM$^-$ cell fraction were positive for EpCAM (data not shown), suggesting that these spheroids were derived from contaminated residual EpCAM$^+$ cells by FACS sorting. All spheroid cells maintained EpCAM expression while half of the attached cells lost EpCAM expression when the EpCAM$^+$ fraction was cultured for 14 days (Figure 4*E*). Most spheroid cells also abundantly expressed proliferating cell nuclear antigen (PCNA), implying active cell proliferation (Figure 4*F* and Supplementary movie 2; see supplementary material online at www.gastrojournal.org). Thus, a subset of EpCAM$^+$ cells, but not EpCAM$^-$ cells, can form spheroids.

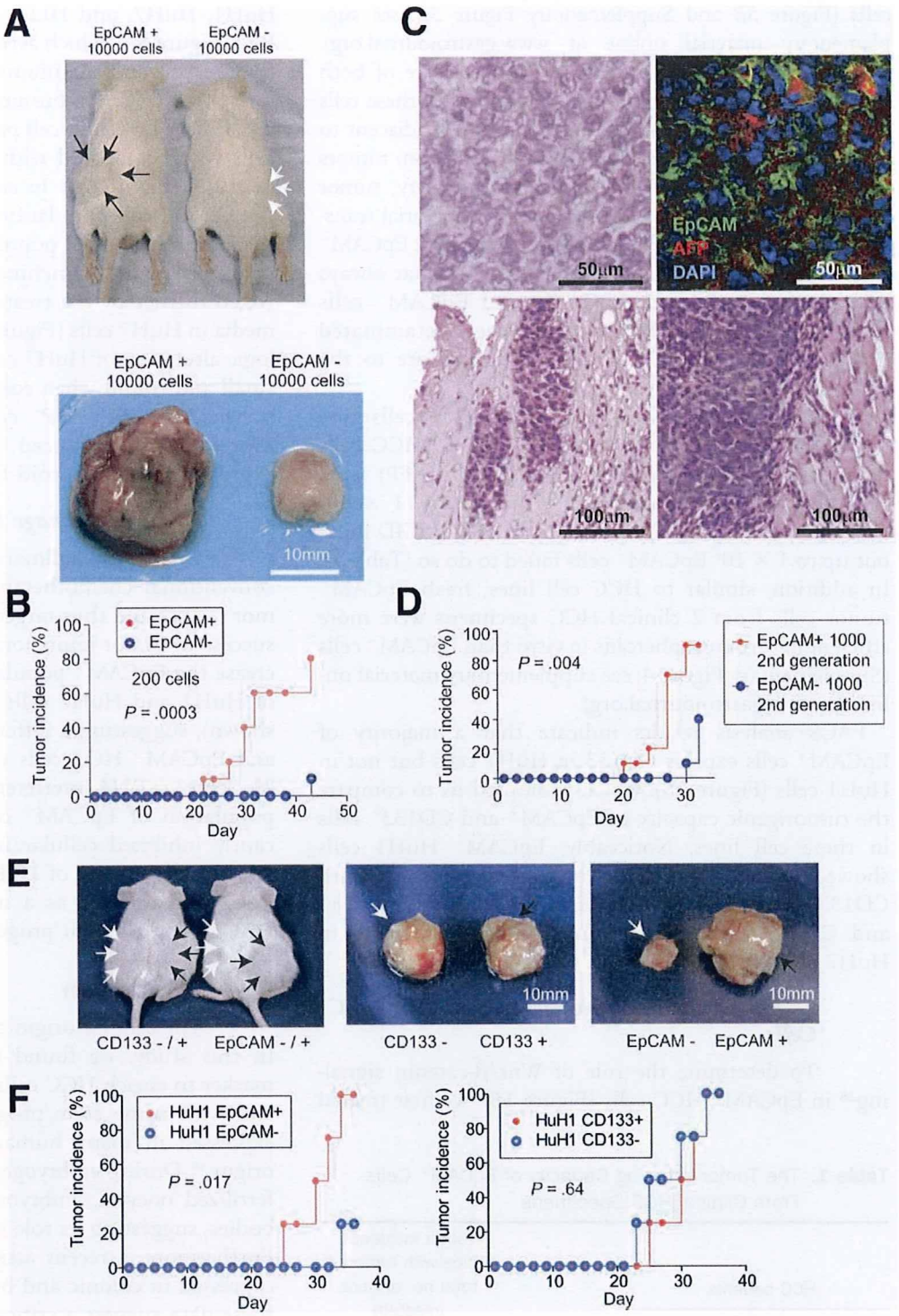

Figure 5. Tumorigenic and invasive potential of EpCAM$^+$ HCC cells. (*A*) Representative NOD/SCID mice (*upper panel*) with subcutaneous tumors (*lower panel*) from EpCAM$^+$ (*black arrows*) or EpCAM$^-$ (*white arrows*) HuH1 cells. (*B*) Tumorigenicity of 200 sorted HuH1 cells. (*C*) Histologic analysis of EpCAM$^+$ HuH1-derived xenografts. H&E staining of a subcutaneous tumor (*left upper panel*) with capsular invasion (*left lower panel*) and muscular invasion (*right lower panel*) and IF of the tumor stained with anti-EpCAM, anti-AFP, and 4′,6-diamidino-2-phenylindole (DAPI) (*right upper panel*) (*scale bar*, 50 μm). (*D*) Tumorigenicity of 1000 sorted cells derived from an EpCAM$^+$ HuH1 xenograft. Data are generated from 10 mice in each group. (*E*) Representative NOD/SCID mice (*left panel*) with subcutaneous tumors from CD133$^+$ (*black arrows*) or CD133$^-$ (*white arrows*) (*middle panel*) and EpCAM$^+$ (black arrows) or EpCAM$^-$ (*white arrows*) (*right panel*) HuH1 cells. (*F*) Tumorigenicity of 1000 HuH1 cells sorted by anti-EpCAM (*left panel*) or anti-CD133 (*right panel*) antibodies.

EpCAM$^+$ HCC Cells as Tumor-Initiating Cells

EpCAM$^+$ HCC cells, but not EpCAM$^-$ HCC cells, could efficiently initiate invasive tumors in NOD/SCID mice (Figure 5). For example, 10,000 EpCAM$^+$ HuH1 cells produced large hypervascular tumors in 100% of mice whereas EpCAM$^-$ cell fractions produced only small and pale-looking tumors in 30% of mice 4 weeks after injection (Figure 5*A* and Supplementary Figure 3*A*; see supplementary material online at www.gastrojournal.org). Similar results were obtained with HuH7 cells (Supplementary Figure 3*B–D*; see supplementary material online at www.gastrojournal.org). As little as 200 EpCAM$^+$ cells could initiate tumors in 8 of 10 injected mice, whereas 200 EpCAM$^-$ cells produced only 1 tumor among 10 injected mice at 6 weeks after transplantation, and the tumor sizes were much larger in the EpCAM$^+$ cells than in the EpCAM$^-$

cells (Figure 5*B* and Supplementary Figure 3*E*; see supplementary material online at www.gastrojournal.org). EpCAM$^+$ cells produced tumors with a mixture of both EpCAM$^+$ and EpCAM$^-$ cells in xenografts, and these cells invaded in the capsule and muscles of the leg adjacent to the tumor (Figure 5*C*). EpCAM$^+$ cells derived from tumors again maintained their tumor-initiating capacity, tumor morphology, and invasive ability in an in vivo serial transplantation experiment (Figure 5*D*). Occasionally, EpCAM$^-$ cell fractions produced a few small tumors that always contained a mixture of EpCAM$^+$ and EpCAM$^-$ cells (data not shown), indicating that the contaminated EpCAM$^+$ cells from FACS sorting contribute to the tumor-initiating ability.

To further validate whether EpCAM$^+$ HCC cells were tumor-initiating cells, we isolated EpCAM$^+$ HCC cells from 2 cases of AFP$^+$ (>600 ng/mL serum AFP) HCC clinical specimens using MACS. Consistently, 1×10^4 EpCAM$^+$ cells could induce tumors in NOD/SCID mice, but up to 1×10^6 EpCAM$^-$ cells failed to do so (Table 1). In addition, similar to HCC cell lines, fresh EpCAM$^+$ tumor cells from 2 clinical HCC specimens were more efficient in forming spheroids in vitro than EpCAM$^-$ cells (Supplementary Figure 4; see supplementary material online at www.gastrojournal.org).

FACS analysis results indicate that a majority of EpCAM$^+$ cells express CD133 in HuH7 cells but not in HuH1 cells (Figure 2*B*), which prompted us to compare the tumorigenic capacity of EpCAM$^+$ and CD133$^+$ cells in these cell lines. Noticeably, EpCAM$^+$ HuH1 cells showed marked tumor-initiating capacity compared with CD133$^+$ HuH1 cells (Figure 5*E* and *F*), whereas EpCAM$^+$ and CD133$^+$ cells had similar tumorigenic ability in HuH7 cells (data not shown).

GSK-3β Inhibition Augments EpCAM$^+$ HCC Cells

To determine the role of Wnt/β-catenin signaling[28] in EpCAM$^+$ HCC cells (Figure 1*B*), we first treated HuH1, HuH7, and HLF cells with a GSK-3β inhibitor BIO (Figure 6*A*), which activates Wnt/β-catenin signaling (Figure 6*B*) and maintains undifferentiation of embryonic stem cells.[38] 6-bromoindirubin-3′-oxime (BIO) increased the EpCAM$^+$ cell population in HuH1 and HuH7 cells when compared with the control methylated BIO (MeBIO) (Figure 6*A*). In contrast, BIO had no effect on the CD90$^+$ cell population, which is more tumorigenic than the CD90$^-$ cell population in HLF (Figure 6*A* and data not shown). Enrichment of EpCAM$^+$ cells was provoked further by the treatment of Wnt10B-conditioned media in HuH7 cells (Figure 6*C*).[34] BIO induced morphologic alteration of HuH7 cells because most cells became small and round when compared with MeBIO and suppressed EpCAM$^-$ AFP$^-$ cell populations (Figure 6*D*). Moreover, BIO induced *TACSTD1*, *MYC*, and *hTERT* expression and spheroid formation (Figure 6*E* and *F*).

Table 1. The Tumor-Initiating Capacity of EpCAM$^+$ Cells From Clinical HCC Specimens

HCC patients				Tumor incidence (mice with tumors/total no. of mice injected)	
No.	% of EpCAM$^+$ HCC cells	Groups	No. of cells injected	2 months	3 months
1	5.2	EpCAM$^+$	1×10^3	0/3	0/3
			1×10^4	2/3	2/3
			1×10^5	2/2	2/2
		EpCAM$^-$	1×10^5	0/3	0/3
			1×10^6	0/2	0/2
2	1.4	EpCAM$^+$	1×10^3	0/2	0/2
			1×10^4	0/1	1/1
		EpCAM$^-$	1×10^4	0/3	0/3
			1×10^5	0/2	0/2

EpCAM Blockage by RNA Interference

One of the hallmarks of CSCs is its resistance to conventional chemotherapeutic agents resulting in tumor relapse and thus targeting CSCs is critical to achieve successful tumor remission. Consistently, 5-FU could increase the EpCAM$^+$ population and spheroid formation of HuH1 and HuH7 cells (Figure 7*A* and *B*) (data not shown), suggesting a differential sensitivity of EpCAM$^+$ and EpCAM$^-$ HCC cells to 5-FU. In contrast, EpCAM blockage via RNA interference dramatically decreased the population of EpCAM$^+$ cells (Figure 7*C*), and significantly inhibited cellular invasion, spheroid formation, and tumorigenicity of HuH1 cells (Figure 7*D–F*). Thus, EpCAM may serve as a molecular target to eliminate HCC cells with stem/progenitor cell features.

Discussion

The cellular origin of HCC is currently in debate. In this study, we found that EpCAM can serve as a marker to enrich HCC cells with tumor-initiating ability and with some stem/progenitor cell traits. EpCAM is expressed in many human cancers with an epithelial origin.[39] During embryogenesis, EpCAM is expressed in fertilized oocytes, embryonic stem cells, and embryoid bodies, suggesting its role in early stage embryogenesis.[40] Furthermore, a recent article indicated that EpCAM is expressed in colonic and breast CSCs.[41] Taken together, these data suggest a critical role of EpCAM in CSCs as well as embryonic and somatic stem cells. Consistently, we found that EpCAM expression is regulated by Wnt/β-catenin signaling[29] and tumorigenic and highly invasive HpSC-HCC is orchestrated by a subset of cells expressing EpCAM and AFP with stem cell–like features and self-renewal and differentiation capabilities regulated by Wnt/β-catenin signaling (this study). Thus, EpCAM may be a common gene expressed in undifferentiated normal cells and HCCs with activated Wnt/β-catenin signaling. It may act as a downstream molecule

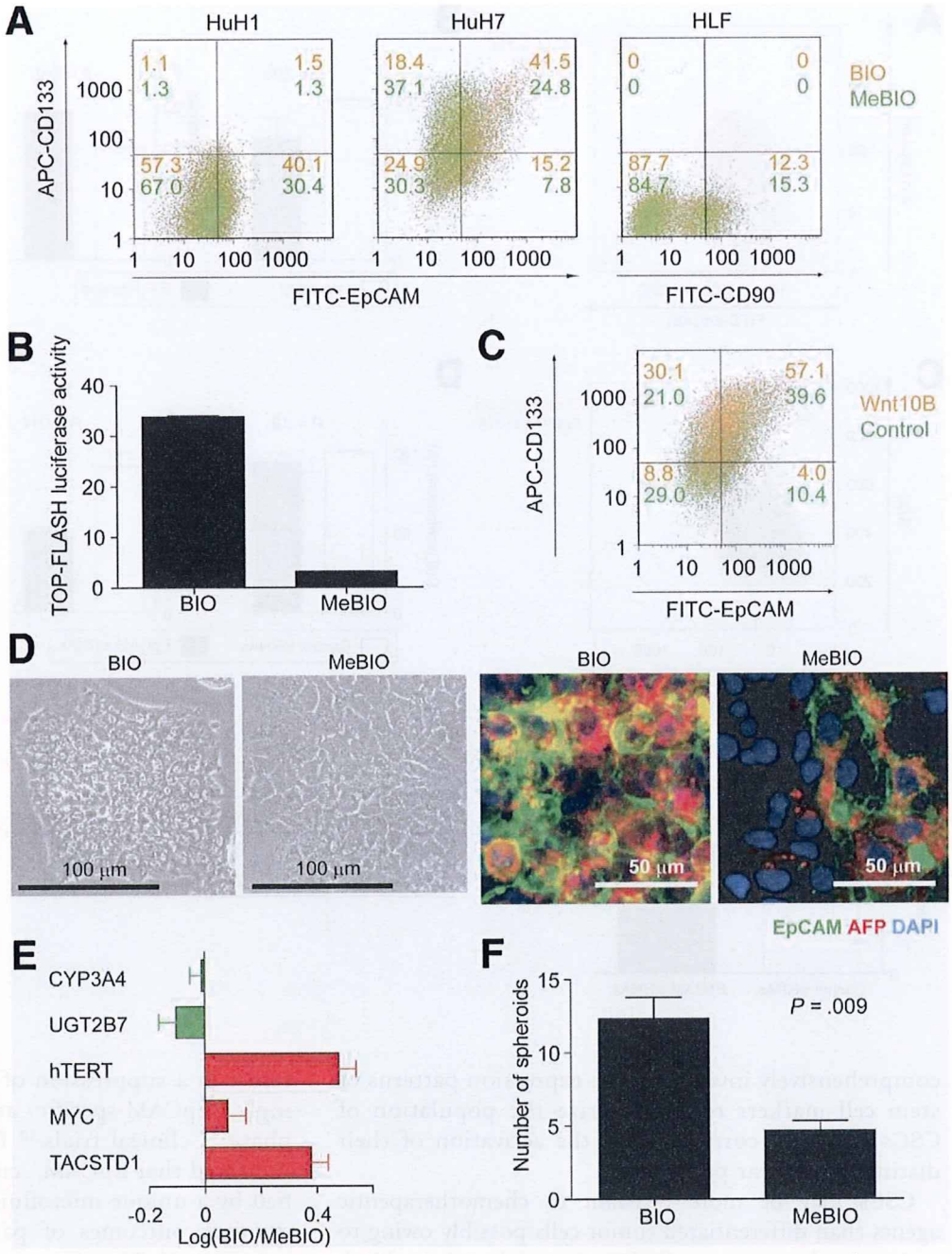

Figure 6. Wnt/β-catenin signaling augments EpCAM$^+$ HCC cells. (*A*) Flow cytometer analysis of HuH1, HuH7, and HLF cells treated with 2 μmol/L of BIO (*orange*) or MeBIO (*green*) for 10 days and stained with anti-EpCAM, anti-CD133 and anti-CD90 antibodies. (*B*) TOP-FLASH luciferase assays of HuH7 cells treated with 2 μmol/L of BIO or MeBIO. (*C*) Flow cytometer analysis of HuH7 cells cultured in normal media (Dulbecco's modified Eagle medium supplemented with 10% FBS) or Wnt10B conditioned media (details are described in the Materials and Methods section). Cells were cultured in each medium for 2 weeks. (*D*) Representative phase-contrast images (*left panel*: *scale bar*, 100 μm) or IF images (*right panel*: *scale bar*, 50 μm) of HuH7 cells treated with 2 μmol/L of BIO or MeBIO for 14 days. (*E*) Quantitative reverse transcription-polymerase chain reaction analysis of representative HpSC-HCC–related genes in HuH7 cells treated with 2 μmol/L of BIO or MeBIO for 14 days. (*F*) Spheroid formation assay of HuH7 cells treated with 2 μmol/L of BIO or MeBIO for 14 days (mean ± SD). FITC, fluorescein isothiocyanate.

to maintain HCC stemness and serve as a good marker for HCC initiating cells.

CD133 or CD90 have been used to identify potential hepatic CSCs.[35,42] CD133 is expressed in normal and malignant stem cells of the neural, hematopoietic, epithelial, hepatic, and endothelial lineages,[23,43,44] suggesting that CD133 is also a common marker to detect normal cells and CSCs. Captivatingly, EpCAM expression overlaps with CD133 expression in normal human colon tissues and colorectal cancer tissues, yet CD133$^+$ and CD133$^-$ cells are equally tumorigenic.[45] Similarly, we found that EpCAM$^+$ and EpCAM$^-$ HuH1 cells equally expressed CD133, but only EpCAM$^+$ cells developed large hypervascular tumors. Our data suggest that EpCAM may be a better marker than CD133 to enrich HCC tumor-initiating cells from AFP$^+$ tumors. We also found that CD90 expression was limited to HCC cell lines that are EpCAM$^-$ AFP$^-$, and Wnt/β-catenin signaling had little effect on CD90$^+$ cell enrichment. These results suggest that the expression patterns of various stem cell markers in tumor-initiating cells with stem/progenitor cell features may be different in each HCC subtype, possibly owing to the heterogeneity of activated signaling pathways in normal stem/progenitor cells where these tumor-initiating cells may originate. Therefore, it would be useful to

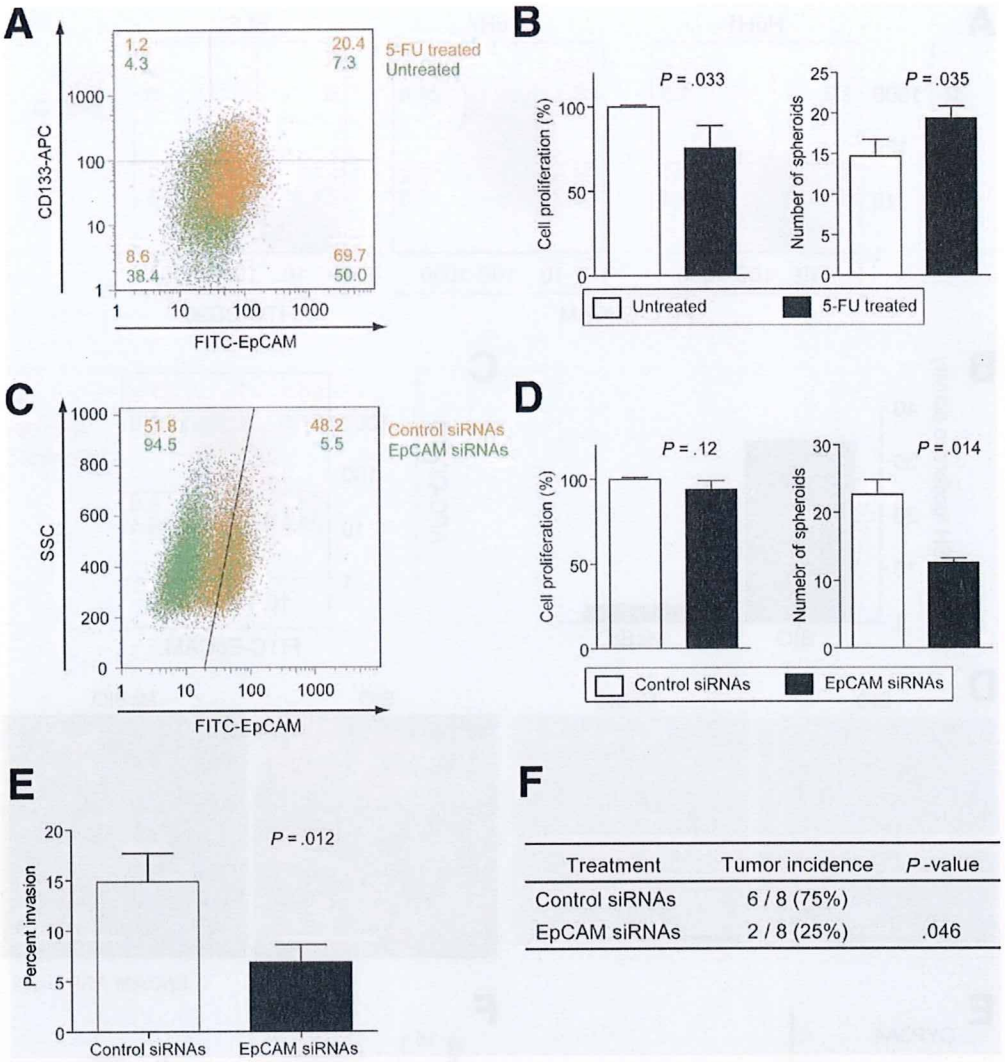

Treatment	Tumor incidence	*P*-value
Control siRNAs	6 / 8 (75%)	
EpCAM siRNAs	2 / 8 (25%)	.046

Figure 7. EpCAM blockage inhibits the tumorigenic and invasive capacity of EpCAM$^+$ HCC cells. (*A*) Enrichment of EpCAM$^+$ cells after 5-FU treatment. HuH1 cells refer as control or without treatment (*green*) or treated with 2 μg/mL of 5-FU (*orange*) for 3 days and analyzed by FACS using anti-EpCAM and anti-CD133 antibodies. (*B*) Spheroid formation of HuH1 cells treated with 2 μg/mL of 5-FU for 3 days. (*C*) FACS analysis of HuH1 cells treated with a control siRNA (orange) or EpCAM-specific siRNA (*green*) at day 3 after transfection. (*D*) Spheroid formation or (*E*) invasive capacity ofEpCAM$^+$ HuH1 cells transfected with a control siRNA or EpCAM-specific siRNA. Experiments were performed in triplicate and the data are shown as mean ± SD. (*D*) siRNAs. (*F*) Inhibition of tumor formation in vivo by EpCAM gene silencing. EpCAM$^+$ HuH1 cells were transfected with siRNA oligos and 1000 cells were injected 24 hours after transfection.

comprehensively investigate the expression patterns of stem cell markers to characterize the population of CSCs that may correlate with the activation of their distinct molecular pathways.

CSCs may be more resistant to chemotherapeutic agents than differentiated tumor cells possibly owing to an increased expression of adenosine triphosphate–binding cassette transporters and anti-apoptotic proteins.[4] Thus, the development of an effective strategy to target CSC pools together with conventional chemotherapies is essential to eradicate a tumor mass.[14] By blocking the programs that activate self-renewal and/or inhibit asymmetric division, CSC features could be destemmed.[46,47] Consistently, EpCAM blockage could inhibit cellular invasion and tumorigenicity of EpCAM$^+$ HCC cells, revealing the feasibility of targeting a CSC marker to destem CSC features. EpCAM may induce c-Myc,[48] a common molecular node activated in HpSC-HCC.[27] c-Myc, together with Oct3/4, Sox2, and Klf4, can induce pluripotent stem cells from adult fibroblasts.[49] It is possible that EpCAM blockage to inhibit hepatic CSCs may result in a suppression of c-Myc signaling. Encouragingly, EpCAM-specific antibodies are currently in phase II clinical trials.[50] Furthermore, a recent study indicated that EpCAM$^+$ circulating tumor cells identified by a unique microfluidic platform can be used to monitor outcomes of patients undergoing systemic treatment.[51] Therefore, it may be useful to combine EpCAM antibodies with conventional chemotherapy to target both CSCs and non-CSCs for the treatment of HCC.

Supplementary Data

Note: To access the supplementary material accompanying this article, visit the online version of *Gastroenterology* at www.gastrojournal.org, and at doi: 10.1053/j.gastro.2008.12.004.

References

1. Fialkow PJ. Clonal origin of human tumors. Biochim Biophys Acta 1976;458:283–321.

2. Heppner GH. Tumor heterogeneity. Cancer Res 1984;44:2259–2265.
3. Hanahan D, Weinberg RA. The hallmarks of cancer. Cell 2000; 100:57–70.
4. Jordan CT, Guzman ML, Noble M. Cancer stem cells. N Engl J Med 2006;355:1253–1261.
5. Clarke MF, Dick JE, Dirks PB, et al. Cancer stem cells—perspectives on current status and future directions: AACR Workshop on cancer stem cells. Cancer Res 2006;66:9339–9344.
6. Potter VR. Phenotypic diversity in experimental hepatomas: the concept of partially blocked ontogeny. The 10th Walter Hubert Lecture. Br J Cancer 1978;38:1–23.
7. Sell S. Cellular origin of cancer: dedifferentiation or stem cell maturation arrest? Environ Health Perspect 1993;101(Suppl 5): 15–26.
8. Wicha MS, Liu S, Dontu G. Cancer stem cells: an old idea—a paradigm shift. Cancer Res 2006;66:1883–1890.
9. Al Hajj M, Wicha MS, Benito-Hernandez A, et al. Prospective identification of tumorigenic breast cancer cells. Proc Natl Acad Sci U S A 2003;100:3983–3988.
10. Singh SK, Hawkins C, Clarke ID, et al. Identification of human brain tumour initiating cells. Nature 2004;432:396–401.
11. Bonnet D, Dick JE. Human acute myeloid leukemia is organized as a hierarchy that originates from a primitive hematopoietic cell. Nat Med 1997;3:730–737.
12. Ricci-Vitiani L, Lombardi DG, Pilozzi E, et al. Identification and expansion of human colon-cancer-initiating cells. Nature 2007; 445:111–115.
13. O'Brien CA, Pollett A, Gallinger S, et al. A human colon cancer cell capable of initiating tumour growth in immunodeficient mice. Nature 2007;445:106–110.
14. Dean M, Fojo T, Bates S. Tumour stem cells and drug resistance. Nat Rev Cancer 2005;5:275–284.
15. Rich JN. Cancer stem cells in radiation resistance. Cancer Res 2007;67:8980–8984.
16. Parkin DM, Bray F, Ferlay J, et al. Global cancer statistics, 2002. CA Cancer J Clin 2005;55:74–108.
17. Sell S, Pierce GB. Maturation arrest of stem cell differentiation is a common pathway for the cellular origin of teratocarcinomas and epithelial cancers. Lab Invest 1994;70:6–22.
18. Thorgeirsson SS, Grisham JW. Hepatic stem cells. Semin Liver Dis 2003;23:301.
19. Thorgeirsson SS, Grisham JW. Molecular pathogenesis of human hepatocellular carcinoma. Nat Genet 2002;31:339–346.
20. Lee JS, Heo J, Libbrecht L, et al. A novel prognostic subtype of human hepatocellular carcinoma derived from hepatic progenitor cells. Nat Med 2006;12:410–416.
21. Sigal SH, Brill S, Fiorino AS, et al. The liver as a stem cell and lineage system. Am J Physiol 1992;263:G139–G148.
22. Schmelzer E, Wauthier E, Reid LM. The phenotypes of pluripotent human hepatic progenitors. Stem Cells 2006;24:1852–1858.
23. Schmelzer E, Zhang L, Bruce A, et al. Human hepatic stem cells from fetal and postnatal donors. J Exp Med 2007;204:1973–1987.
24. Dan YY, Riehle KJ, Lazaro C, et al. Isolation of multipotent progenitor cells from human fetal liver capable of differentiating into liver and mesenchymal lineages. Proc Natl Acad Sci U S A 2006;103:9912–9917.
25. Zaret KS. Regulatory phases of early liver development: paradigms of organogenesis. Nat Rev Genet 2002;3:499–512.
26. Shafritz DA, Oertel M, Menthena A, et al. Liver stem cells and prospects for liver reconstitution by transplanted cells. Hepatology 2006;43:S89–S98.
27. Yamashita T, Forgues M, Wang W, et al. EpCAM and alpha-fetoprotein expression defines novel prognostic subtypes of hepatocellular carcinoma. Cancer Res 2008;68:1451–1461.
28. Reya T, Clevers H. Wnt signalling in stem cells and cancer. Nature 2005;434:843–850.
29. Yamashita T, Budhu A, Forgues M, et al. Activation of hepatic stem cell marker EpCAM by Wnt-β-catenin signaling in hepatocellular carcinoma. Cancer Res 2007;67:10831–10839.
30. Budhu A, Forgues M, Ye QH, et al. Prediction of venous metastases, recurrence and prognosis in hepatocellular carcinoma based on a unique immune response signature of the liver microenvironment. Cancer Cell 2006;10:99–111.
31. Ye QH, Qin LX, Forgues M, et al. Predicting hepatitis B virus-positive metastatic hepatocellular carcinomas using gene expression profiling and supervised machine learning. Nat Med 2003;9:416–423.
32. Wu CG, Forgues M, Siddique S, et al. SAGE transcript profiles of normal primary human hepatocytes expressing oncogenic hepatitis B virus X protein. FASEB J 2002;16:1665–1667.
33. Kubota H, Reid LM. Clonogenic hepatoblasts, common precursors for hepatocytic and biliary lineages, are lacking classical major histocompatibility complex class I antigen. Proc Natl Acad Sci U S A 2000;97:12132–12137.
34. Yoshikawa H, Matsubara K, Zhou X, et al. WNT10B functional dualism: beta-catenin/Tcf-dependent growth promotion or independent suppression with deregulated expression in cancer. Mol Biol Cell 2007;18:4292–4303.
35. Yang ZF, Ho DW, Ng MN, et al. Significance of CD90(+) cancer stem cells in human liver cancer. Cancer Cell 2008;13:153–166.
36. Dontu G, Abdallah WM, Foley JM, et al. In vitro propagation and transcriptional profiling of human mammary stem/progenitor cells. Genes Dev 2003;17:1253–1270.
37. Fang D, Nguyen TK, Leishear K, et al. A tumorigenic subpopulation with stem cell properties in melanomas. Cancer Res 2005; 65:9328–9337.
38. Sato N, Meijer L, Skaltsounis L, et al. Maintenance of pluripotency in human and mouse embryonic stem cells through activation of Wnt signaling by a pharmacological GSK-3-specific inhibitor. Nat Med 2004;10:55–63.
39. Balzar M, Winter MJ, de Boer CJ, et al. The biology of the 17-1A antigen (Ep-CAM). J Mol Med 1999;77:699–712.
40. Trzpis M, McLaughlin PM, de Leij LM, et al. Epithelial cell adhesion molecule: more than a carcinoma marker and adhesion molecule. Am J Pathol 2007;171:386–395.
41. Dalerba P, Dylla SJ, Park IK, et al. Phenotypic characterization of human colorectal cancer stem cells. Proc Natl Acad Sci U S A 2007;104:10158–10163.
42. Ma S, Chan KW, Hu L, et al. Identification and characterization of tumorigenic liver cancer stem/progenitor cells. Gastroenterology 2007;132:2542–2556.
43. Yin AH, Miraglia S, Zanjani ED, et al. AC133, a novel marker for human hematopoietic stem and progenitor cells. Blood 1997;90: 5002–5012.
44. Fargeas CA, Corbeil D, Huttner WB. AC133 antigen, CD133, prominin-1, prominin-2, etc.: prominin family gene products in need of a rational nomenclature. Stem Cells 2003;21:506–508.
45. Shmelkov SV, Butler JM, Hooper AT, et al. CD133 expression is not restricted to stem cells, and both CD133+ and CD133- metastatic colon cancer cells initiate tumors. J Clin Invest 2008; 118:2111–2120.
46. Hill RP, Perris R. "Destemming" cancer stem cells. J Natl Cancer Inst 2007;99:1435–1440.
47. Piccirillo SG, Reynolds BA, Zanetti N, et al. Bone morphogenetic proteins inhibit the tumorigenic potential of human brain tumour-initiating cells. Nature 2006;444:761–765.
48. Munz M, Kieu C, Mack B, et al. The carcinoma-associated antigen EpCAM upregulates c-myc and induces cell proliferation. Oncogene 2004;23:5748–5758.

49. Takahashi K, Tanabe K, Ohnuki M, et al. Induction of pluripotent stem cells from adult human fibroblasts by defined factors. Cell 2007;131:861–872.
50. Chaudry MA, Sales K, Ruf P, et al. EpCAM an immunotherapeutic target for gastrointestinal malignancy: current experience and future challenges. Br J Cancer 2007;96:1013–1019.
51. Nagrath S, Sequist LV, Maheswaran S, et al. Isolation of rare circulating tumour cells in cancer patients by microchip technology. Nature 2007;450:1235–1241.

Received March 9, 2008. Accepted December 1, 2008.

Reprint requests

Address requests for reprints to: Xin Wei Wang, PhD, Liver Carcinogenesis Section, Laboratory of Human Carcinogenesis, Center for Cancer Research, National Cancer Institute, 37 Convent Drive, Building 37, Room 3044A, MSC 4258, Bethesda, Maryland 20892-4258. e-mail: xw3u@nih.gov; fax: (301) 496-0497.

Acknowledgments

Microarray data are available publicly at http://www.ncbi.nlm.nih.gov/geo/ (accession number: GSE5975).

The authors thank Drs Curtis Harris and Sharon Pine for critical readings of the manuscript; Ms Barbara Taylor and Dr Susan Garfield for technical assistance; Drs Ali Brivanlou (Rockefeller University), Steve Strom (University of Pittsburgh), and Bert Vogelstein (Johns Hopkins University) for generously providing their research materials.

Conflicts of interest

The authors disclose no conflicts.

Funding

The authors disclose the following: This work was supported in part by the Intramural Research Program of the Center for Cancer Research, the US National Cancer Institute. Dr Yang, Dr HY Wang, Dr Jia, Dr Ye, Dr Qin, and Dr Tang were supported by research grants from the China National Natural Science Foundation for Distinguished Young Scholars (30325041) and the China National "863" R&D High-Tech Key Project (2002BA711A02-4). Dr Reid was supported by a sponsored research grant from Vesta Therapeutics (Research Triangle Park, NC), National Institutes of Health grants (RO1 AA014243 and RO1 IP30-DK065933), and a US Department of Energy grant (DE-FG02-02ER-63477). Sponsors had no role in the study design, data collection, analysis, and interpretation. Dr Yamashita, Dr Ji, Dr Budhu, Dr Forgues, Dr Yang, Dr Wang, Dr Jia, Dr Ye, Dr Wauthier, Dr Minato, Dr Honda, Dr Kaneko, and Dr Wang disclose no conflicts.

ELSEVIER

Journal of Hepatology 48 (2008) 736–742

Journal of Hepatology

www.elsevier.com/locate/jhep

The presence of steatosis and elevation of alanine aminotransferase levels are associated with fibrosis progression in chronic hepatitis C with non-response to interferon therapy☆

Masayuki Kurosaki[1], Kotaro Matsunaga[1], Itsuko Hirayama[1], Tomohiro Tanaka[1], Mitsuaki Sato[1], Nobutoshi Komatsu[1], Naoki Umeda[1], Takanori Hosokawa[1], Ken Ueda[1], Kaoru Tsuchiya[1], Hiroyuki Nakanishi[1], Jun Itakura[1], Yasuhiro Asahina[1], Shozo Miyake[1], Nobuyuki Enomoto[2], Namiki Izumi[1,*]

[1]*Division of Gastroenterology and Hepatology, Musashino Red Cross Hospital, 1-26-1 Kyonan-cho, Musashino-shi, Tokyo 180-8610, Japan*
[2]*First Department of Internal Medicine, University of Yamanashi, Yamanashi, Japan*

***Background/Aims*: Interferon (IFN) therapy leads to regression of hepatic fibrosis in chronic hepatitis C patients who achieve a sustained virologic response (SVR), while the beneficial effect is limited in those who fail to do so. The aim of the present study was to define factors associated with progression of fibrosis in patients who do not achieve a SVR.**

***Methods*: Fibrosis staging scores were compared between paired liver biopsies before and after IFN in 97 chronic hepatitis C patients who failed therapy. The mean interval between biopsies was 5.9 years. Factors associated with progression of fibrosis were analyzed.**

***Results*: Fibrosis progressed in 23%, remained unchanged in 47% and regressed in 29%. Steatosis and a high average alanine aminotransferase (ALT) between biopsies were independent factors for progression of fibrosis with risk ratios of 5.53 and 4.48, respectively. Incidence and yearly rate of progression of fibrosis was 64% and 0.22 ± 0.29 fibrosis units per year in those with both risk factors compared to 8% and −0.04 ± 0.17 fibrosis units per year in those negative for both factors.**

***Conclusions*: Hepatic steatosis and elevated ALT levels are risk factors for progression of fibrosis in chronic hepatitis C patients who fail to achieve a SVR to IFN therapy and therefore may be therapeutic targets to halt the potentially progressive disease.**

***Keywords*: Steatosis; ALT; Fibrosis**

1. Introduction

Hepatitis C virus (HCV) is a major cause of chronic liver disease worldwide. Mortality associated with HCV infection results from the development of liver cirrhosis and hepatocellular carcinoma, which now is the leading indication for liver transplantation [1]. Treatment with interferon (IFN), alone or in combination with ribavirin (RBV), can eradicate HCV infection in some patients, leading to sustained nor-

Received 20 July 2007; received in revised form 8 October 2007; accepted 17 December 2007; available online 26 February 2008
Associate Editor: J.G. McHutchison

☆ The authors who have taken part in the research of this paper declared that they do not have a relationship with the manufactures of the drug involved either in the past or present and they did not receive funding from the manufactures to carry out their research. They did not receive funding from any source to carry out this study.

* Corresponding author. Tel.: +81 422 32 3111; fax: +81 422 32 9551.
E-mail address: nizumi@musashino.jrc.or.jp (N. Izumi).

0168-8278/$34.00
doi:10.1016/j.jhep.2007.12.025

malization of liver function, improvement of hepatic inflammation and fibrosis and a decreased risk of the development of hepatocellular carcinoma [2,3]. The problem is that only 50% of patients achieve a sustained virological response (SVR) to therapy even with the most highly developed regimens of IFN [4,5]. The remaining patients who fail to clear the virus are left with the risk of progressive disease. In order to halt this potentially progressive disease, there is a need to establish an effective target of therapeutic intervention independent of antiviral therapy. Therefore, it is important to define risk factors for the progression of fibrosis among chronic hepatitis C patients who do not achieve a SVR to IFN therapy.

Several factors that may affect the rate of progression of fibrosis have been investigated extensively, including older age at infection, male gender, obesity, heavy alcohol consumption, and a high grade of necroinflammation [6–8]. Several cross-sectional and longitudinal studies suggest that hepatic steatosis, which is a common histological feature of chronic hepatitis C [9], influences the progression of hepatic fibrosis [10–14], while other studies did not find such an association [15–18]. Besides these conflicting results, no study to date has reported the effect of steatosis on longitudinal progression of fibrosis among patients who fail to respond to IFN therapy. Therefore, we studied factors associated with progression of fibrosis in those who failed IFN therapy by comparing paired pre-treatment and post-treatment liver biopsies.

2. Methods

2.1. Patients

The aim of the study was to identify risk factors associated with progression of fibrosis in chronic hepatitis C patients who failed to achieve a SVR to IFN therapy. To be included in this retrospective study, patients had to have undergone liver biopsy before and after therapy, been treated with IFN and not achieved a SVR. Patients with alcohol consumption of more than 20 g per day, co-infected with HBV or HIV, and those with another known aetiology of liver disease, such as autoimmune hepatitis or metabolic disorders, were excluded. A database of patients who had undergone liver biopsy at Musashino Red Cross Hospital between 1990 and 2004 was reviewed retrospectively and a total of 1241 chronic hepatitis C patients treated with IFN were identified; of these, 407 had a SVR and 834 had not achieved a SVR. Among those with treatment failure, 104 fulfilled the above criteria but seven patients with cirrhosis before treatment were excluded because the endpoint of the study was progression of fibrosis. Therefore, this study cohort consisted of 97 patients. In these patients, second liver biopsies were performed before the second course of IFN therapy. Otherwise, there were no standardized indications for the second liver biopsy which may be the limitation of our study. Demographic characteristics of patients at the time of initial biopsy are shown in Table 1. The time between the paired biopsies was 5.9 years on average, with a range of 1.2–11.6 years. The median interval between first biopsy and IFN therapy was 3 days (range 2–93 days), and that between completion of IFN therapy and second biopsy was 5.4 years (range 0.8–11.2 years). Laboratory tests were performed monthly or bimonthly in all patients and all measurements were taken at our single hospital.

Table 1
Demographic characteristics of patients

Number of patients	97
Age (years)	52 ± 9
Gender: male/female	50/47
BMI (kg/m^2)	23.9 ± 3.2 (median 24.0, range19–33)
BMI <25/25–30/30 ⩽ (kg/m^2)	55/37/5
Route of transmission	
Blood transfusion/unknown	38/59
Duration of infection (years)	30.4 ± 9.2 (median 33.5, range 3–48)
Genotype 1b/2a/2b	85/4/8
Serum HCV-RNA (Meq/ml)	7.7 ± 9.7
Pretreatment AST (IU/l)	73 ± 40
Pretreatment ALT (IU/l)	104 ± 69
Pretreatment GGT (IU/l)	51 ± 44
Histological variables at first biopsy	
Stage of fibrosis 1/2/3	33/38/26
Grade of activity 0/1/2/3	15/36/41/5
Grade of steatosis 0/1/2/3	21/37/25/14
Size of steatosis macro/micro/mixed	16/17/64
Localization of steatosis centrilobular/diffuse	3/94

BMI, body mass index; AST, aspartate aminotransferase, normal range is 7–38 IU; ALT, alanine aminotransferase, normal range is 4–43 IU/l; GGT, gamma-glutamyltransferase, normal range is 0–73 IU/l; macro, macro-vesicular steatosis; micro, micro-vesicular steatosis.

2.2. Histological evaluation

Median length of biopsy specimen and number of portal tracts were 13.0 mm (range 10–40 mm) and 12 (range 6–34). All liver biopsy specimens were evaluated separately by three independent pathologists who were blinded to the clinical data. If there was discordance, the scores assigned by two pathologists were used for the analysis. Fibrosis and activity were scored according to the METAVIR scoring system [19]. Fibrosis was staged on a scale of 0–4: F0 (no fibrosis), F1 (mild fibrosis: portal fibrosis without septa), F2 (moderate fibrosis: few septa), F3 (severe fibrosis: numerous septa without cirrhosis) and F4 (cirrhosis). Activity of necroinflammation was graded on a scale of 0–3: A0 (no activity), A1 (mild activity), A2 (moderate activity) and A3 (severe activity). Percentage of steatosis was quantified by determining the average proportion of hepatocytes affected by steatosis and was graded on a scale of 0–3: grade 0 (no steatosis), grade 1 (0–9%), grade 2 (10–29%), and grade 3 (over 30%). Size of steatosis was categorized into micro-vesicular, macro-vesicular and mixed types. Localization of steatosis was categorized into either centrilobular or diffuse pattern. Definition of changes in the grade of steatosis was as follows: worsening as 1 point or more increase, improvement as 1 point or more decrease, and stability as no change.

2.3. Changes in fibrosis-staging score overtime

Changes in progression of fibrosis were defined as follows: progression of fibrosis was defined as a 1 point or more increase, regression as a 1 point or more decrease and stability as no change in the METAVIR fibrosis-staging score. In addition, because the time between paired biopsies was variable, the yearly rate of progression of fibrosis was calculated as the change in fibrosis-staging score divided by the time between paired biopsies, as originally described by Poynard et al. [6].

2.4. Statistical analysis

The STAT View software package was used for statistical analysis. Categorical data were analyzed using the Fisher's exact test. Continuous variables were compared with the Student's t test. Variables that were statistically significant in univariate analysis were included in multivariate analysis using logistic regression analysis. The Kaplan–Meier method and log-rank test were used to analyze the time to occurrence of fibrosis progression. A p-value of less than 0.05 was considered statistically significant.

3. Results

3.1. Factors associated with the initial stage of fibrosis (cross-sectional study)

All three pathologists assigned the same score in 85% of patients for fibrosis staging and 95% of patients for steatosis-grading. In cases with discordance, at least two pathologists assigned the same scale. The stage of fibrosis in the initial liver biopsy was F1 in 33, F2 in 38 and F3 in 26 patients. Various clinical factors were analyzed in association with the advanced stage of fibrosis. As a result, the presence of F3 fibrosis was associated with older age, (51 ± 9 in F1–2 vs. 55 ± 9 in F3, $p = 0.03$), higher grade of histological activity (A2–3 was 35% in F1–2 vs. 84% in F3, $p = 0.0001$) and higher grade of steatosis (steatosis grade 2–3 was 34% in F1–2 vs. 58% in F3, $p = 0.04$).

The grade of steatosis was 0 in 21, 1 in 37, 2 in 25 and 3 in 14 patients. A higher grade of steatosis was associated with female gender (the male/female ratio was 35/23 in grade 0–1 vs. 15/24 in grade 2–3, $p = 0.04$), increased BMI (BMI over 25 kg/m^2 was 31% in grade 0–1 vs. 62% in grade 2–3, $p = 0.006$), and higher grade of histological activity (A2–3 was 38% in grade 0–1 vs. 62% in grade 2–3, $p = 0.03$). Multivariate logistic regression analysis revealed that increased BMI and female gender were independent factors associated with a high grade of steatosis (Table 2).

Table 2
Multivariate logistic regression analysis of factors associated with hepatic steatosis

	Odds	95% C.I.	p Value
BMI			
$\geqslant$25 kg/m^2	4.23	1.63–10.95	0.003
Gender			
Female	2.75	1.06–7.14	0.04
Activity grade			
2–3	2.30	0.85–6.26	0.10
Fibrosis stage			
3	1.63	0.53–4.97	0.39

3.2. Change in fibrosis-staging scores over time (longitudinal study)

Fibrosis staging progressed in 23% (progression by 2 points in 5% and 1 point in 18%), remained unchanged in 47% and regressed in 29% (regression by 2 points in 2% and 1 point in 27%). At first liver biopsy, laparoscopy was performed in 73 patients and the presence of cirrhosis (F4) was carefully excluded. In another 24 patients, the possibility of mis-diagnosis of F4 as F3 remains. However, the incidence of fibrosis progression did not differ according to the initial stage of fibrosis (21.2% in F1, 26.3% in F2 and 19.2% in F3, $p = 0.78$) which indicates that misdiagnosis of F4 as F3 at initial biopsy is unlikely.

Among various factors, as shown in Table 3, a higher grade of steatosis, higher levels of ALT and AST (average value for the period between the paired liver biopsies) were associated with progression of fibrosis. Since there was significant correlation between ALT and AST levels ($r = 0.684$, $p < 0.0001$), these two variables could not be analyzed together in multivariate analysis.

Table 3
Factors associated with the progression of fibrosis over time

	Progression $n = 22$	Non-progression $n = 75$	p Value
Gender: male/female	9/13	41/34	0.33
Age at biopsy: <60/$\geqslant$60 years	14/8	59/16	0.17
HCV genotype: 1b/non-1b	19/3	66/9	0.99
BMI: <25/$\geqslant$25 kg/m^2	11/11	44/31	0.48
Duration of infection (years)	32.1 ± 5.2	29.9 ± 10.0	0.56
Activity on first biopsy			
Grade: 0–1/2–3	8/14	43/32	0.10
Steatosis on first biopsy			
Grade: 0–1/2–3	6/16	52/23	0.001
Size: macro/micro/mixed	4/4/14	12/13/50	0.96
Location: centrilobular/diffuse	1/21	2/73	0.54
Evolution of steatosis			
Worsening/improvement/stable	2/2/18	9/8/58	0.09
Average ALT: <100/$\geqslant$100 IU/l	13/9	67/8	0.003
Average AST: <75/$\geqslant$75 IU/l	10/12	61/14	0.002
Interval between biopsies (years)	5.1 ± 3.2	6.2 ± 2.4	0.09
Interval between completion of IFN and second biopsy (years)	4.6 ± 3.2	5.7 ± 2.4	0.10
Treatment regimen			
RBV–/RBV+	22/0	71/4	0.27
Response to IFN			
Relapser/non-responder	16/6	53/22	0.99
Evolution of weight			
Gain/loss/stable	5/8/9	29/21/25	0.38

macro, macro-vesicular steatosis; micro, micro-vesicular steatosis; RBV–, interferon monotherapy; RBV+, interferon plus ribavirin combination therapy.
Duration of infection was determined in 38 patients whose source of infection was blood transfusion.

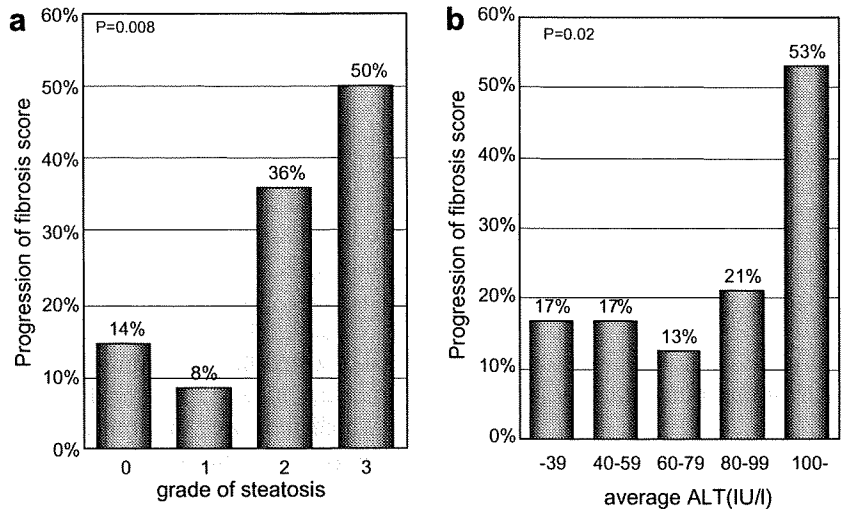

Fig. 1. Progression of fibrosis stage, hepatic steatosis and the average level of ALT. The progression of the fibrosis score over time is illustrated using bar charts. (a) Steatosis grades of 2 or 3 at initial liver biopsy were associated with the increased progression of fibrosis over time. (b) High average ALT levels during the observation period were associated with progression of fibrosis at the threshold of 100 IU/l.

Thus, average level of ALT was used for the following analysis. The probability of progression of fibrosis was 14%, 8%, 36% and 50% in patients with steatosis grades of 0, 1, 2 and 3, respectively ($p = 0.008$), and 17%, 17%, 13%, 21% and 53% in patients with average ALT values of <40, 40–59, 60–79, 80–99 and over 100 IU/l, respectively ($p = 0.02$) (Fig. 1). Multivariate logistic regression analysis revealed that these two were independent risk factors associated with the progression of fibrosis with risk ratios of 5.14 for steatosis ($p = 0.004$) and 5.21 for ALT ($p = 0.01$) (Table 4).

When patients were categorized in terms of these two risk factors, the incidence of progression of fibrosis was as high as 64% in those with both risk factors, compared to 8% in those negative for these factors. Conversely, the incidence of fibrosis regression was only 9% in those with both risk factors, compared to 37% in those negative for these factors ($p = 0.0003$) (Fig. 2).

In order to adjust for the effect of variable intervals between paired biopsies, the yearly rate of progression of fibrosis was calculated as the change in the fibrosis-staging score divided by the time between paired biopsies. The average of all patients was 0.02 ± 0.22 fibrosis units per year. Again, a higher grade of steatosis ($p = 0.004$) and higher average level of ALT ($p = 0.0005$) were associated with a higher rate of progression of fibrosis (Table 5). In addition, the yearly rate of progression of fibrosis was 0.22 ± 0.29 fibrosis units per year in those with both risk factors, 0.12 ± 0.37 in those with elevated ALT alone, 0.05 ± 0.16 in those with steatosis alone and -0.05 ± 0.17 in those negative for these two factors ($p = 0.001$). Time to progression of fibrosis at second biopsy was also analyzed by the Kaplan–Meier method. The cumulative probabilities of progression of fibrosis at five years were 58% in those with both risk factors, 33% in those with elevated ALT alone, 18% in those with steatosis alone and 2% in those negative for these two factors ($p < 0.0001$) (Fig. 3).

Table 4
Multivariate logistic regression analysis of factors associated with progression of fibrosis over time

	Odds	95% C.I.	p Value
Steatosis grade ≥2	5.14	1.67–15.77	0.004
Average ALT ≥100 IU/l	5.21	1.49–18.20	0.01

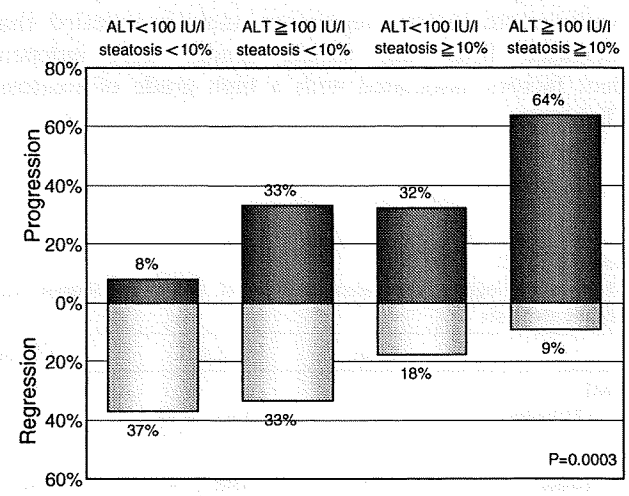

Fig. 2. Evolution of fibrosis stage in terms of risk factors. Patients were categorized into four groups according to the presence or absence of two risk factors. The upper bar chart (dark gray) indicates the progression of fibrosis while the lower bar chart (light gray) indicates the regression of fibrosis.

Table 5
Factors associated with the yearly rate of fibrosis progression

	n	Mean	SD	*p* Value
Gender				
Male	50	−0.01	0.19	0.12
Female	47	0.06	0.23	
Age at biopsy				
<60 years	73	−0.0002	0.21	0.06
⩾60 years	24	0.10	0.23	
HCV genotype				
1b	83	0.02	0.20	0.37
non-1b	14	0.08	0.32	
BMI				
<25 kg/m^2	53	0.004	0.24	0.32
⩾25 kg/m^2	44	0.05	0.19	
Steatosis on first biopsy				
0–1	58	−0.03	0.20	0.004
2–3	39	0.10	0.21	
Activity on first biopsy				
0–1	51	−0.001	0.21	0.24
2–3	46	0.05	0.22	
Fibrosis on first biopsy				
1–2	71	0.03	0.20	0.43
3	26	−0.01	0.25	
Average ALT between paired biopsies				
<100 IU/l	80	−0.01	0.17	0.0005
⩾100 IU/l	17	0.18	0.31	

4. Discussion

In the present study, we found that a higher grade of hepatic steatosis at baseline and a higher average value of ALT are independent risk factors for the progression of fibrosis over time in chronic hepatitis C patients who fail to achieve a SVR to IFN therapy. These two factors may be involved in promoting the progression of fibrosis. The association between steatosis and progression of fibrosis in untreated patients had been suggested by previous studies but this study is the first to demonstrate a similar association for treated patients. These findings are particularly important to establish a rationale for identifying therapeutic targets to halt potentially progressive disease independent of antiviral therapy.

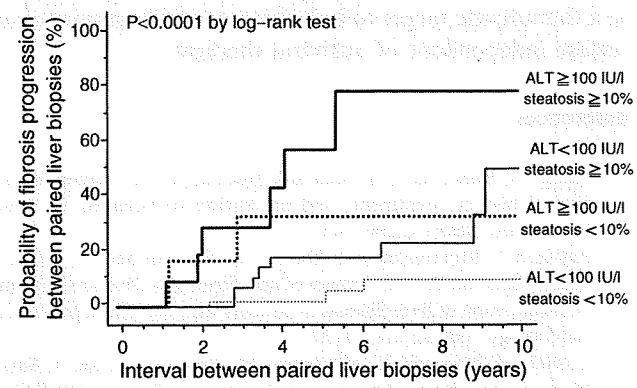

Fig. 3. Probability of fibrosis progression according to the presence of risk factors. Patients were categorized into four groups according to the presence or absence of two risk factors and the time to progression of fibrosis was analyzed.

There have been many studies that analyzed the association between steatosis and progression of liver fibrosis in HCV-infected patients, and the majority have shown a positive association [10–13], including a large scale meta-analysis [14]. However, some studies did not report this association [15–18]. There are two possible reasons for these conflicting results. First, longitudinal studies, rather than cross-sectional studies, are particularly important in the analysis of the role of steatosis in time-dependent progression of hepatic fibrosis, because cross-sectional studies involve patients with an unknown duration of steatosis. Three of four longitudinal studies that analyzed the progression of fibrosis through paired biopsies in untreated patients showed that the presence or worsening of steatosis was associated with the progression of fibrosis [12,13,20], and the probability of progression of fibrosis was significantly related to the grade of steatosis [13]. In one study, however, progression of fibrosis was correlated with older age, periportal necroinflammation and ALT elevations but not with steatosis [17]. Interestingly, steatosis was associated with older age, higher body mass index and ALT elevations in that study, indicating an indirect association of steatosis and fibrosis progression. The authors assumed that steatosis was the result rather than the cause of inflammation. This observation highlights the second reason for the controversies over a correlation between the presence of steatosis and progression of fibrosis, that is, there are so many confounding factors associated with both steatosis and fibrosis progression such as older age, advanced stage of fibrosis, higher degree of inflammation, elevated ALT, increased body mass index and insulin resistance. Because it is very difficult to prove a causal relationship between these confounding factors through clinical observations, steatosis may be a hallmark of the progression of fibrosis but it is unclear whether the effect of steatosis on progression of fibrosis is direct or mediated by other confounding factors.

Hepatic steatosis is a common pathological finding in patients with chronic hepatitis C [9]. Because the proportion of patients with steatosis is higher than would be expected from a chance association, a direct role of HCV in the pathogenesis of steatosis is suggested, at least in some patients with genotype 3 infection [21]. Furthermore, other observations suggest that steatosis may be metabolic; it is correlated with a high body mass index, visceral adiposity and insulin resistance, especially in non-3a genotypes and metabolic steatosis also is correlated with progression of fibrosis [11,22]. The

most reliable evidence that metabolic steatosis is associated with progression of fibrosis is shown by a study indicating that weight reduction in patients with chronic hepatitis C leads to a reduction in steatosis and an improvement in fibrosis, despite the persistence of HCV infection. A reduction in steatosis was significantly associated with a decrease in stellate cell activation and regression of hepatic fibrosis in 56% of patients. Thus, weight reduction may provide an important new adjunct treatment strategy for patients with chronic hepatitis C [23]. A recent study showed that the administration of pioglitazone led to metabolic and histological improvement in subjects with non-alcoholic steatohepatitis [24]. Whether amelioration of insulin resistance could improve steatosis and fibrosis in chronic hepatitis C awaits future investigation.

The mechanism by which steatosis could aggravate hepatic fibrosis in chronic hepatitis C patients remains largely hypothetical. Steatosis related insulin resistance may contribute to hyperinsulinemia and increased hepatic expression of connective tissue growth factor leading to progression of fibrosis [25]. Alternatively, a steatohepatitis-like pathway may be involved where steatosis requires a second hit for progression to fibrosis [26]. The most likely candidate is an oxidative stress with subsequent lipid peroxidation which is reported to correlate with the stage of fibrosis [27]. Another important candidate is an antiviral inflammatory response. It is reported that steatotic liver has increased susceptibility to inflammatory response [28] and that a higher grade of steatosis is correlated with a higher degree of inflammation or elevated ALT [14,15,17]. Higher degree of inflammation or elevated ALTs are associated with the progression of fibrosis [29,30], but hepatic steatosis may be responsible for the amplification of hepatic inflammation and vice versa, and the coexistence of these two factors may lead to further progression of fibrosis, as in patients with non-alcoholic steatohepatitis. In our study, average value of ALT between two biopsies was associated with fibrosis progression, whereas histological inflammation at first liver biopsy was not. The reason for this discordance may be explained by the dynamic process of hepatic necroinflammation. Severity of histological inflammation at the time of biopsy may not reflect subsequent inflammation process, whereas average value of regularly determined ALT may reflect entire fluctuation of hepatic inflammation. If so, our finding may support the hypothesis that co-operation of steatosis as the first hit and dynamic process of hepatic inflammation as the second hit promotes fibrosis progression. On the other hand, elevation of ALT may not be a mere reflection of hepatic inflammation so much as hepatocellular death such as apoptosis. Since it is reported that apoptotic caspase activation is elevated in HCV-associated steatosis [31] and that steatotic liver has increased susceptibility to apoptosis [28], elevation of ALT may also reflect an apoptosis amplified by steatosis which may lead to fibrosis progression.

Regardless of the precise mechanism, the results of the present study suggest that lowering of ALT levels may be beneficial in preventing progression of fibrosis in patients who failed to achieve a SVR. In our population, all patients received 24 weeks of IFN therapy and none received long-term maintenance therapy aiming to ameliorate hepatic inflammation. However, we speculate that amelioration of hepatic inflammation and lowering ALT levels by long-term IFN may prevent fibrosis progression in patients who remain viremic since it has been reported that IFN slowed the natural progression of fibrosis in patients who failed IFN therapy when the rate of progression of fibrosis after IFN therapy was compared to the estimated rate of progression before therapy [2,32], and that treatment duration was associated with the reduction of fibrosis independent of virological response [2]. Another possible approach to lower ALT levels may be the use of ursodeoxycholic acid, which has been reported to induce an almost 30% decrease in serum ALT levels [33,34]. The long-term efficacy of therapies targeted to the reduction of hepatic fibrosis needs future verification.

Some factors related to fibrosis progression in previous studies such as obesity [35] and worsening of steatosis [20] were not significant in our study. In our study where the majority of the population had normal body weight and very few had obesity (BMI $\geqslant 30\ kg/m^2$), impact of increased BMI on fibrosis progression may not be evaluated. Also, a smaller number of patients with worsening of steatosis (11.3% in present study and 34% in previous study [20]) may be the reason for the discrepancy. This may be due to difference in patient selection since no patients in that study had antiviral treatment between two biopsies.

In conclusion, the presence of hepatic steatosis and elevated ALT levels are risk factors for progression of fibrosis in chronic hepatitis C patients who failed to achieve a SVR to IFN therapy. These two factors may be a therapeutic target to halt the potentially progressive disease independent of antiviral therapy.

References

[1] Liang TJ, Rehermann B, Seeff LB, Hoofnagle JH. Pathogenesis, natural history, treatment, and prevention of hepatitis C. Ann Intern Med 2000;132:296–305.

[2] Poynard T, McHutchison J, Davis GL, Esteban-Mur R, Goodman Z, Bedossa P, et al. Impact of interferon alfa-2b and ribavirin on progression of liver fibrosis in patients with chronic hepatitis C. Hepatology 2000;32:1131–1137.

[3] Yoshida H, Shiratori Y, Moriyama M, Arakawa Y, Ide T, Sata M, et al. Interferon therapy reduces the risk for hepatocellular carcinoma: national surveillance program of cirrhotic and noncirrhotic patients with chronic hepatitis C in Japan. IHIT Study Group. Inhibition of Hepatocarcinogenesis by Interferon Therapy. Ann Intern Med 1999;131:174–181.

[4] Manns MP, McHutchison JG, Gordon SC, Rustgi VK, Shiffman M, Reindollar R, et al. Peginterferon alfa-2b plus ribavirin compared with interferon alfa-2b plus ribavirin for initial treatment of chronic hepatitis C: a randomised trial. Lancet 2001;358:958–965.
[5] Fried MW, Shiffman ML, Reddy KR, Smith C, Marinos G, Goncales Jr FL, et al. Peginterferon alfa-2a plus ribavirin for chronic hepatitis C virus infection. N Engl J Med 2002;347:975–982.
[6] Poynard T, Bedossa P, Opolon P. Natural history of liver fibrosis progression in patients with chronic hepatitis C. The OBSVIRC, METAVIR, CLINIVIR, and DOSVIRC groups. Lancet 1997;349:825–832.
[7] Marcellin P, Asselah T, Boyer N. Fibrosis and disease progression in hepatitis C. Hepatology 2002;36:S47–S56.
[8] Alberti A, Vario A, Ferrari A, Pistis R. Review article: chronic hepatitis C – natural history and cofactors. Aliment Pharmacol Ther 2005;22 Suppl 2:74–78.
[9] Lefkowitch JH, Schiff ER, Davis GL, Perrillo RP, Lindsay K, Bodenheimer Jr HC, et al. Pathological diagnosis of chronic hepatitis C: a multicenter comparative study with chronic hepatitis B. The Hepatitis Interventional Therapy Group. Gastroenterology 1993;104:595–603.
[10] Hourigan LF, Macdonald GA, Purdie D, Whitehall VH, Shorthouse C, Clouston A, et al. Fibrosis in chronic hepatitis C correlates significantly with body mass index and steatosis. Hepatology 1999;29:1215–1219.
[11] Adinolfi LE, Gambardella M, Andreana A, Tripodi MF, Utili R, Ruggiero G. Steatosis accelerates the progression of liver damage of chronic hepatitis C patients and correlates with specific HCV genotype and visceral obesity. Hepatology 2001;33:1358–1364.
[12] Westin J, Nordlinder H, Lagging M, Norkrans G, Wejstal R. Steatosis accelerates fibrosis development over time in hepatitis C virus genotype 3 infected patients. J Hepatol 2002;37:837–842.
[13] Fartoux L, Chazouilleres O, Wendum D, Poupon R, Serfaty L. Impact of steatosis on progression of fibrosis in patients with mild hepatitis C. Hepatology 2005;41:82–87.
[14] Leandro G, Mangia A, Hui J, Fabris P, Rubbia-Brandt L, Colloredo G, et al. Relationship between steatosis, inflammation, and fibrosis in chronic hepatitis C: a meta-analysis of individual patient data. Gastroenterology 2006;130:1636–1642.
[15] Asselah T, Boyer N, Guimont MC, Cazals-Hatem D, Tubach F, Nahon K, et al. Liver fibrosis is not associated with steatosis but with necroinflammation in French patients with chronic hepatitis C. Gut 2003;52:1638–1643.
[16] Hui JM, Sud A, Farrell GC, Bandara P, Byth K, Kench JG, et al. Insulin resistance is associated with chronic hepatitis C virus infection and fibrosis progression [corrected]. Gastroenterology 2003;125:1695–1704.
[17] Perumalswami P, Kleiner DE, Lutchman G, Heller T, Borg B, Park Y, et al. Steatosis and progression of fibrosis in untreated patients with chronic hepatitis C infection. Hepatology 2006;43:780–787.
[18] Conjeevaram HS, Kleiner DE, Everhart JE, Hoofnagle JH, Zacks S, Afdhal NH, et al. Race, insulin resistance and hepatic steatosis in chronic hepatitis C. Hepatology 2007;45:80–87.
[19] Bedossa P, Poynard T. An algorithm for the grading of activity in chronic hepatitis C. The METAVIR Cooperative Study Group. Hepatology 1996;24:289–293.
[20] Castera L, Hezode C, Roudot-Thoraval F, Bastie A, Zafrani ES, Pawlotsky JM, et al. Worsening of steatosis is an independent factor of fibrosis progression in untreated patients with chronic hepatitis C and paired liver biopsies. Gut 2003;52:288–292.
[21] Mihm S, Fayyazi A, Hartmann H, Ramadori G. Analysis of histopathological manifestations of chronic hepatitis C virus infection with respect to virus genotype. Hepatology 1997;25:735–739.
[22] Fartoux L, Poujol-Robert A, Guechot J, Wendum D, Poupon R, Serfaty L. Insulin resistance is a cause of steatosis and fibrosis progression in chronic hepatitis C. Gut 2005;54:1003–1008.
[23] Hickman IJ, Clouston AD, Macdonald GA, Purdie DM, Prins JB, Ash S, et al. Effect of weight reduction on liver histology and biochemistry in patients with chronic hepatitis C. Gut 2002;51:89–94.
[24] Belfort R, Harrison SA, Brown K, Darland C, Finch J, Hardies J, et al. A placebo-controlled trial of pioglitazone in subjects with nonalcoholic steatohepatitis. N Engl J Med 2006;355:2297–2307.
[25] Paradis V, Perlemuter G, Bonvoust F, Dargere D, Parfait B, Vidaud M, et al. High glucose and hyperinsulinemia stimulate connective tissue growth factor expression: a potential mechanism involved in progression to fibrosis in nonalcoholic steatohepatitis. Hepatology 2001;34:738–744.
[26] Day CP, James OF. Steatohepatitis: a tale of two "hits"? Gastroenterology 1998;114:842–845.
[27] Paradis V, Mathurin P, Kollinger M, Imbert-Bismut F, Charlotte F, Piton A, et al. In situ detection of lipid peroxidation in chronic hepatitis C: correlation with pathological features. J Clin Pathol 1997;50:401–406.
[28] Walsh MJ, Vanags DM, Clouston AD, Richardson MM, Purdie DM, Jonsson JR, et al. Steatosis and liver cell apoptosis in chronic hepatitis C: a mechanism for increased liver injury. Hepatology 2004;39:1230–1238.
[29] Mathurin P, Moussalli J, Cadranel JF, Thibault V, Charlotte F, Dumouchel P, et al. Slow progression rate of fibrosis in hepatitis C virus patients with persistently normal alanine transaminase activity. Hepatology 1998;27:868–872.
[30] Ghany MG, Kleiner DE, Alter H, Doo E, Khokar F, Promrat K, et al. Progression of fibrosis in chronic hepatitis C. Gastroenterology 2003;124:97–104.
[31] Seidel N, Volkmann X, Langer F, Flemming P, Manns MP, Schulze-Osthoff K, et al. The extent of liver steatosis in chronic hepatitis C virus infection is mirrored by caspase activity in serum. Hepatology 2005;42:113–120.
[32] Shiffman ML, Hofmann CM, Contos MJ, Luketic VA, Sanyal AJ, Sterling RK, et al. A randomized, controlled trial of maintenance interferon therapy for patients with chronic hepatitis C virus and persistent viremia. Gastroenterology 1999;117:1164–1172.
[33] Omata M, Yoshida H, Toyota J, Tomita E, Nishiguchi S, Hayashi N, et al. A large-scale, multicentre, double-blind trial of ursodeoxycholic acid in patients with chronic hepatitis C. Gut 2007;56:1747–1753.
[34] Takano S, Ito Y, Yokosuka O, Ohto M, Uchiumi K, Hirota K, et al. A multicenter randomized controlled dose study of ursodeoxycholic acid for chronic hepatitis C. Hepatology 1994;20:558–564.
[35] Ortiz V, Berenguer M, Rayon JM, Carrasco D, Berenguer J. Contribution of obesity to hepatitis C-related fibrosis progression. Am J Gastroenterol 2002;97:2408–2414.